University of Stavanger

Faculty of Science and Technology

BACHELOR`S THESIS

Study program/Specialization: Bachelor of Engineering - Geoscience and Energy Resources	Fall semester, 2023 Open / Restricted access
Writer: Line Skorpe Aasprong	…… (Writer's signature)
Faculty supervisor(s): Nestor Fernando Cardozo Diaz Anaëlle Guillevic	
Thesis title: Geothermal gradient from well log data in the Froan and Gimsan basins, Norwegian Sea	
Credits (ECTS): 20	
Key words: Norwegian Continental Shelf Thermal Conductivity Heat Conduction Geothermal	Pages: 59 Stavanger, 12.12.2023

Geothermal gradient from well log data in the Froan and Gimsan basins, Norwegian Sea

December 12, 2023

Abstract

This thesis reconstructs geothermal gradients in the Froan and Gimsan basins of the Norwegian Sea, utilizing well log data to derive a more accurate representation of the thermal regime of these basins. The study challenges the traditional linear approximation of geothermal gradients, emphasizing the complexity of formation-based thermal properties and subsurface temperature regimes. By incorporating a variety of geological parameters, the study aims to deepen our understanding of subsurface temperature variations and enhance insights into the geothermal potential of these regions.

A combination of geological, geophysical, and temperature data is employed to reconstruct the geothermal gradients through a straightforward one-dimensional (1D) heat conduction model. This model, which assumes a steady-state heat flow, is used to observe the impact of thermal conductivity on the temperature regime. The primary objective is to obtain realistic thermal conductivity values from well logs, utilizing a method developed by Fuchs et al. (2015). These thermal conductivity values are then used to reconstruct the geothermal gradient in the well, assuming constant heat flow and no heat from radiogenic elements. These are of course over-simplifications, but still they allowed me to estimate the relative variation of geothermal gradient over the area.

The findings indicate significant deviations from the linear thermal gradient model, providing a more realistic understanding of the variation in subsurface thermal conductivities. This understanding has important implications for geothermal energy exploration, suggesting more complex thermal behavior than previously assumed. The study places greater emphasis on thermal conductivity findings over thermal gradients due to some data limitations and the inherent simplifications required in the modeling process. However, the estimated thermal gradients are still worth looking, at least on a relative basis. This work highlights the need for more comprehensive data collection and advanced modeling techniques in future research to accurately assess the geothermal potential of these areas.

Contents

Introduction

The transfer of heat from the Earth's interior is primarily derived from the residual energy of the processes of planetary formation and radioactive decay (English et al., 2023). Near the surface, heat is predominantly transferred by conduction, and geothermal gradients are highest there (Boden, 2017). Regions with particularly high subsurface temperatures are often associated with active tectonics, such as the Pacific Ring of Fire (Elders & Moore, 2016). However, elevated temperature gradients can also be found in sedimentary basins due to the insulating properties of sedimentary rocks, combined with continuous heat flux and radiogenic heat production (English et al., 2023).

The investigation of subsurface temperature regimes has long been a cornerstone of oil and gas exploration and is increasingly important for geothermal energy prospects. Geothermal potential exist from gradients of 30°C per kilometer and above, with shallow depths suitable for heating applications, and depths of 4-5 km offering sufficient temperatures for power generation (English et al., 2023). The Norwegian Continental Shelf hosts sedimentary basins where geothermal gradients have been estimated to exceed 41.3°C per kilometre (Lundin et al., 2005). The study area is located within the Trøndelag platform and Halten terrace and is proximal to the mainland, with extensive facilities and data due to oil and gas activities. This makes it an interesting area for geothermal exploration.

Problem statement

The common approximation of a linear thermal gradient in sedimentary basins can lead to oversimplistic interpretations of subsurface temperature distributions, as it does not account for the heterogeneity of sediment composition, which can significantly influence heat conduction. While high heat flow is necessary for elevated temperatures, low thermal conductivity can lead to heat accumulation within sedimentary basins, increasing geothermal gradients (Labus & Labus, 2018). Thermal conductivity in sedimentary basins is affected by mineral composition, fluid content, porosity, and other geological factors. Non- sedimentary rocks (basement) , high-quartz sedimentary rocks, or evaporites like salt have higher thermal conductivities compared to shale, coal, or organic-rich sediments. The porosity and nature of pore fillings—whether dry, brine-saturated, or hydrocarbon-bearing—further complicate the assessment of thermal conductivity. Fac-

tors such as grain size, sorting quality, burial depth, and structural setting also impact thermal properties. Hence, the actual temperatures in the subsurface, especially in sedimentary basins, can vary greatly.

Objective

This study aims to enhance the linear geothermal gradient model and derive a more accurate representation of thermal gradients within sedimentary basins and in particular in the study area. By incorporating various geological parameters, this thesis seeks to gain deeper insights into subsurface temperature variations. Although achieving an absolute true gradient is beyond the scope, this study attempts to approximate a more realistic gradient by factoring in thermal conductivity.

Methods

The approach combines geological, geophysical, and temperature data to refine the modeling of thermal gradients. The primary challenge is to derive realistic thermal conductivity values, for which we utilize well log data. By adopting the methodology suggested by Fuchs et al. (2015) to estimate thermal conductivity from well logs, the aim is to obtain an enhanced understanding of the subsurface thermal regime.

Results and analysis

The resulting geothermal gradients suggest significant deviations from the linear model. These deviations are analyzed to identify key factors responsible for their occurrence and discuss implications for the geothermal potential of the area.

Theory

1.1 Earth's temperature regime

1.1.1 Internal heat sources

The collisions forming Earth released substantial amounts of kinetic energy, resulting in the separation of Earth's elements. Iron and nickel settled in the core, while the mantle consists of dense iron and magnesium-rich rocks. The outer crust contains igneous, metamorphic and sedimentary rocks. The igneous rocks of the ocean plates contain more mafic minerals, and those of the continental crust contain more felsic minerals. Temperature distribution within the Earth is affected by this separation of elements. The Earth's core contains heat derived from the preserved energy generated during its formation. The thermal energy that flows from the Earth's core towards the surface is slowed down due to the insulating properties of subsurface rocks, resulting in an uneven temperature distribution with depth depending on the distinct thermal properties of rocks and the plate tectonic setting (Boden, 2017).

Radiation constitutes another primary internal heat source (Boden, 2017). This contribution to heat flow results from the decay of radioactive elements. These elements are prevalent in the crust, but due to the small volume of the crust compared to the mantle, a significant portion of radiogenic heat production originates from the mantle (Boden, 2017).

1.1.2 Linear geothermal gradient

As heat flows from the core towards the surface, the subsurface temperature generally increases with depth. An average geothermal gradient of 30°C per kilometer of depth is a commonly accepted estimate. However, it is important to note that the uneven distribution of heat flow causes significant variations in the thermal gradient (Grotzinger & Jordan, 2014). To calculate the average geothermal gradient in a specific area, we can use equation (1.1) (Rider & Kennedy, 2014):

$$G = \frac{T_{formation} - T_{surface}}{depth} \tag{1.1}$$

G is the average geothermal gradient, which commonly has units of $°C/km$. $T_{formation}$ represents the temperature of the formation, which could be the temperature at the base of a borehole, or the temperature at the base of any other formation. $T_{surface}$ represents the surface temperature, or if in an oceanic area, the sea floor temperature. It can also be the temperature at the top of a formation of interest.

Even though regional heat flow variations are considered when the gradient is computed for a specific area, the assumption of a linear temperature increase with depth does only consider a homogeneous subsurface. To consider the heterogeneity of the formations, other rock-related parameters such as thermal conductivity should be investigated (Rider & Kennedy, 2014).

1.1.3 Heat distribution

The areas exhibiting the highest heat flow are typically located near tectonic plate boundaries or near hotspots within the plates, where significant heat energy from the Earth's core and mantle is released (Boden, 2017).

Depending on temperature, geothermal systems can be divided into high, moderate, and low enthalpy systems. High and moderate systems often are located in high heat flow areas, and low (but sometimes also high and moderate) enthalpy systems exists in low heat flow areas.

Elevated heat flow is commonly observed in deep sedimentary basins, where sediments overlay granitic rocks with high radiogenic heat production (Boden, 2017). In this geological setting, the basement rocks serve as the primary heat source, while the sediments act as insulating layers. The thermal conductivity of rocks, particularly the lower thermal conductivity of sedimentary rocks like shale, plays a crucial role in slowing down the heat transfer process (Rider & Kennedy, 2014). The continuous decay of radioactive isotopes from specific elements in the basement contributes persistently to the heat within these basins. Sedimentary basins can have geothermal potential if temperatures reach 175 – 200 $°C$ at depths of 4 – 5 km (Boden, 2017).

The distribution of heat flow is also influenced by the structural setting. Processes such as extension and faulting lead to the thinning of the lithosphere, bringing the mantle closer to the surface. Additionally, the presence of faults and fractures increases permeability, creating pathways for fluid flow. This enhanced permeability can elevate heat flow within the geological system (Rider & Kennedy, 2014).

1.2 Heat transfer mechanisms

In general, subsurface heat flow is mainly transferred by convection and conduction. Even though radiogenic heat production may affect the temperature regime in the crust, heat radiation as a transport mechanism is typically insignificant in the upper crust (Kauerauf & Hantschel, 2009).

1.2.1 Convection

Convection is a heat transfer mechanism related to the flow of heat mainly from a fluid. As rock properties such as density are affected by temperature, and due to gravity, fluids of higher temperatures rise and flow towards the surface, resulting in convective heat transfer. This mechanism is also dependent on other rock properties such as porosity and permeability. Plate tectonics driven by the internal heat sources also impacts rocks by deformation. Fault structures can increase permeability, so heat flow is also dependent on geologic structures (Boden, 2017).

1.2.2 Conduction

When determining the geothermal gradient in the subsurface, it is crucial to consider heat transfer through conduction, which is the main mechanism in the shallow lithosphere. Conductive heat transfer is related to the transfer of heat due to contact between materials, and it is a result of a temperature difference between two locations. Conduction is controlled by the thermal conductivity of the rock materials involved, and it is influenced by the distance between two locations at different temperatures (Kauerauf & Hantschel, 2009).

Heat conduction is described by Fourier's law:

$$q = -TC \cdot \Delta T \tag{1.2}$$

Here q represents the heat transfer rate, TC denotes the thermal conductivity, and ΔT is the temperature gradient (Fuchs et al., 2015).

Rocks	**TC (W/mK)**
Coal	0.14 - 0.42
Shale	0.4 - 3.0
Marl	1.2 - 2.5
Claystone	0.8 - 1.7
Siltstone	1.5 - 3.0
Limestone	2.0 - 3.4
Dolomite	2.6 - 5.0
Sandstone	2.0 - 5.1
Tuff	0.5 - 2.5
Basalt	1.7 - 2.9
Granite	1.7 - 4.0
Fluids	**TC (W/mK)**
Air	0.03
Water, fresh	0.06
Gas	0.08
Oil	0.15
Ice	2.2
Minerals	**TC (W/mK)**
Mica	2.0 - 2.3
Quartz	7.7
Anhydrite	4.8
Halite	6.5

Table 1.1: Common thermal conductivity values for selected rocks, minerals, and fluids. The values vary due to compositional differences, which makes narrow ranges difficult to estimate. (Bagdassarov, 2021; Fuchs et al., 2015; Labus & Labus, 2018; Rider & Kennedy, 2014; Wang et al., 2021)

Thermal conductivity

The process of conductive heat transfer relies on the material's thermal conductivity (TC), which represents the material's ability to conduct heat. Shales exhibit an insulating effect due to their low thermal conductivity, while rock materials like salt have a high thermal conductivity and facilitate more efficient heat conduction (Rider & Kennedy, 2014). Determining an exact value for the rock thermal conductivity is a complex task, primarily due to significant variations not only among different lithologies but also within them. Thermal conductivity is influenced by factors such as fluid composition, mineral content, and the overall heterogeneity of the rocks (Kauerauf & Hantschel, 2009). As outlined in Table 1.1, there is a great variation of TC values in geologic materials. Consequently, the determination of TC for a specific area often requires the formulation

of certain assumptions and generalizations. Despite these simplifications, estimating accurately thermal conductivity is challenging and time-consuming (Fuchs et al., 2015).

1.3 Study area and geological setting

1.3.1 Study area

The study area is situated within two significant structural provinces in the mid Norwegian Sea: the Halten Terrace, and the Trøndelag Platform (figure 1.1). The area encompasses the southern part of the Trøndelag Platform, including the Froan Basin and Frøya High, and incorporates structural sub-elements of the Halten Terrace, such as the Gimsan Basin. The study area extends to include fault complexes that separate the main provinces, notably the Bremstein fault complex and the Vingleia fault complex, situated on the shallow part of the Halten Terrace (figure 1.1) (Blystad et al., 1995; Færseth, 2021). A map illustraing the well locations used in this study is given in figure 1.2.

1.3.2 Structural setting

The Norwegian Continental Shelf displays the characteristics of a rifted passive continental margin, particularly influenced by the breakup and formation of the North Atlantic in the Norwegian Sea. Separated by about 350 million years, these two plate tectonic events caused notable alterations to the stress regime in the region (Blystad et al., 1995).

In the Late Silurian to Early Devonian, compression arose from the collision between the Baltic and Laurentian plates, leading to the closure of the Iapetus ocean and the Caledonian orogeny (Færseth, 2021). Subsequent to the Iapetus Ocean closure, the stress regime shifted to extensional during the separation of Eurasia and Greenland, persisting until the beginning of the Eocene. Another change in stress regime occurred in the Tertiary, marked by weak compression during Tertiary seafloor spreading (Blystad et al., 1995).

The extension from the Late Devonian to Early Eocene played a significant role in reshaping the continental shelf through faulting and crustal thinning. Three notable rift events occurred during this phase: Permian-Triassic, Middle-Late Jurassic, and Cretaceous-Tertiary (Færseth, 2021). The lithostratigraphic column in figure 1.5 illustrates the timing of syn-rift and post-rift events during this period. The subsequent sections outline key events affecting the study area.

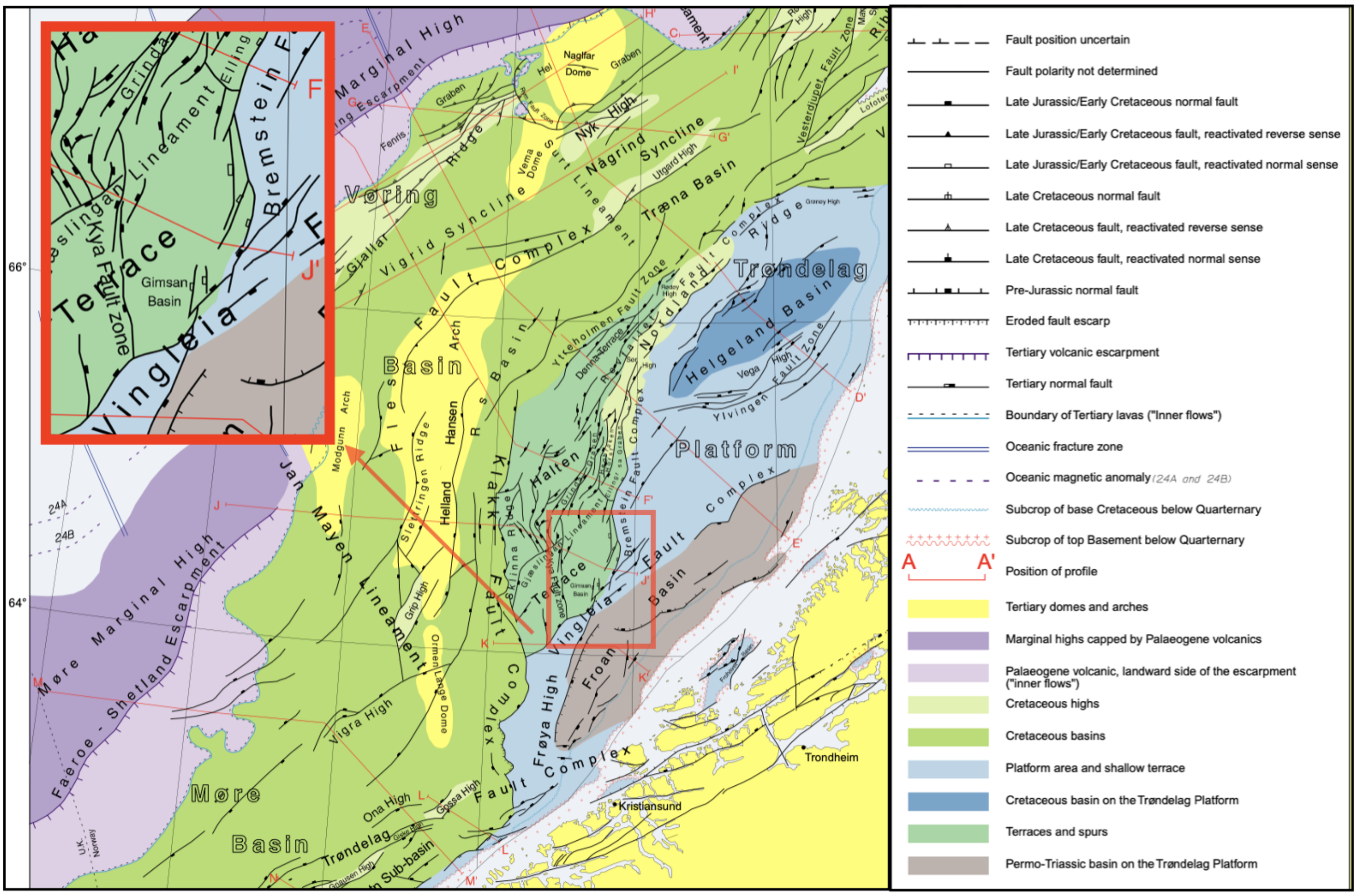

Figure 1.1: Structural elements of the Norwegian Sea and location of the study area in the red rectangle. Modified from NPD Factpages.

Late Permian – Early Triassic Rift event

The Froan Basin was formed as a result of the extensional faulting that occurred during the Late Permian - Early Triassic Rifting. This Permo-Triassic basin is situated within the southern part of the Trøndelag platform, and it is bounded by the Norwegian mainland to the northeast, and a fault system extending southeast towards the Frøya High, as displayed in the geological profile of figure 1.3. Other deep rift basins were possibly also formed between the Trøndelag Platform and the Halten terrace, but their sediments were removed by erosion (Riis et al., 2014). A major unconformity indicates deep erosion during the mid Triassic (Brekke & Riis, 1987).

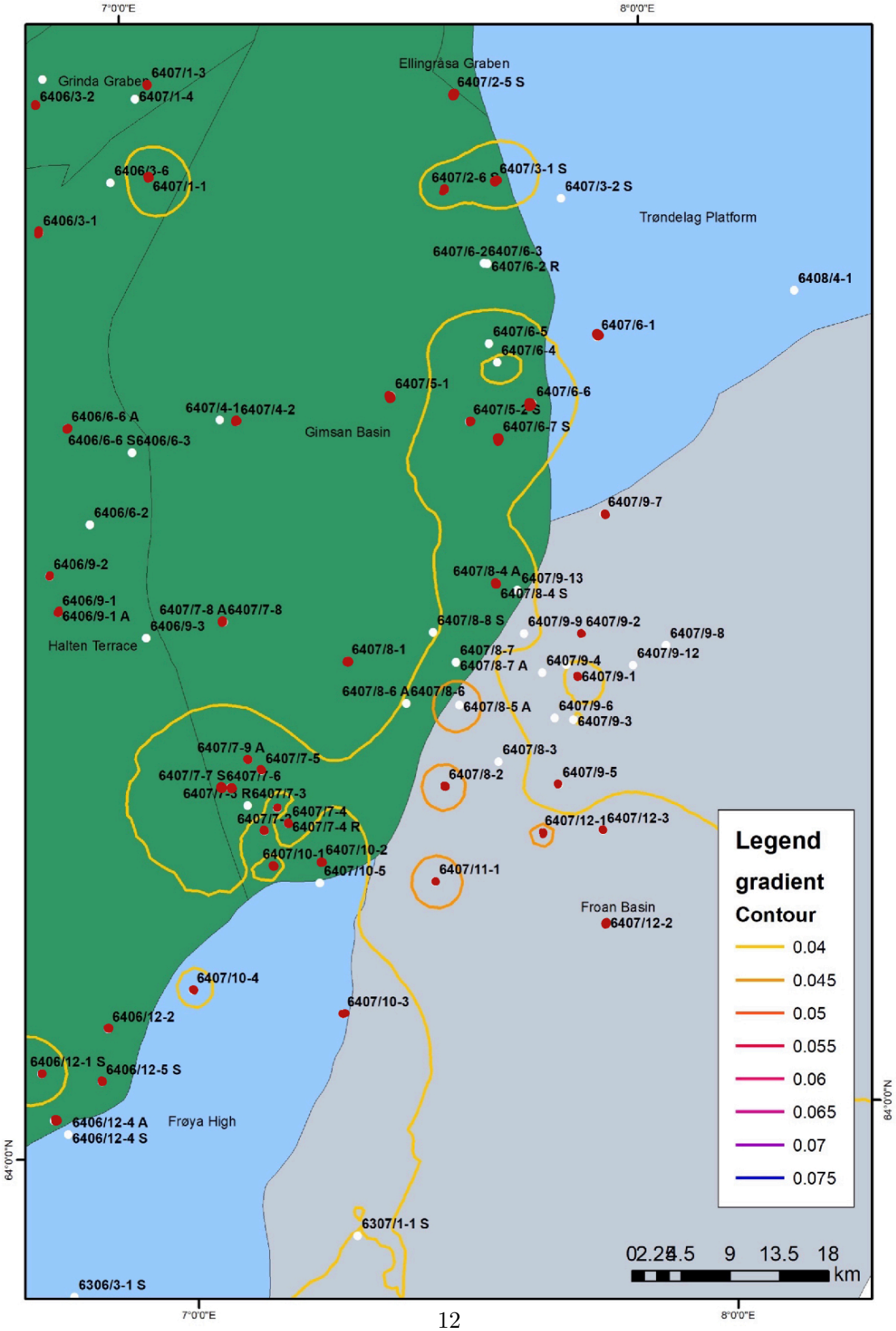

Figure 1.2: Map of the study area, including location of wells and structural provinces. The red dots are the wells that are used in this study.

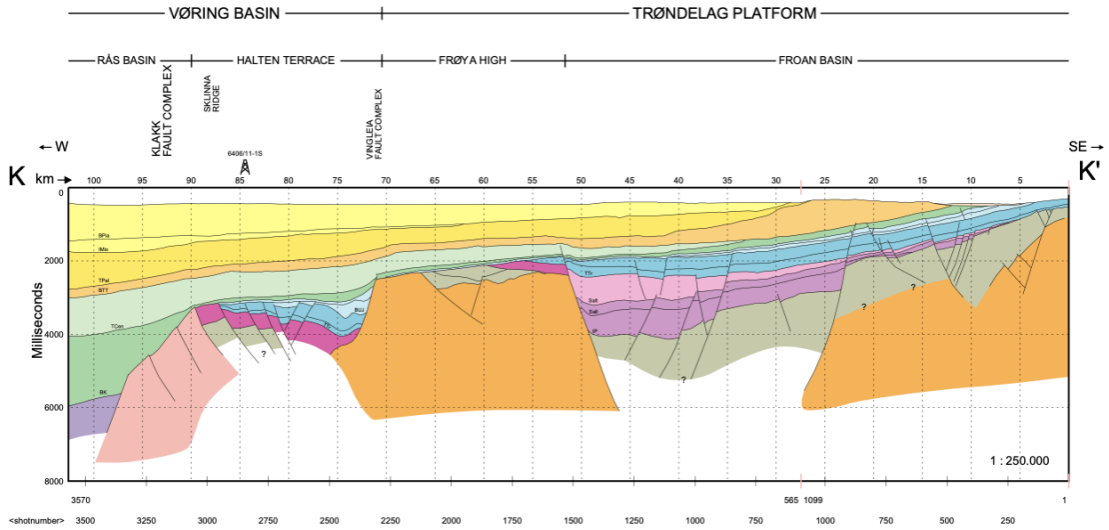

Figure 1.3: Cross section along line K-K' in Figure 1. Modified from NPD Factpages.

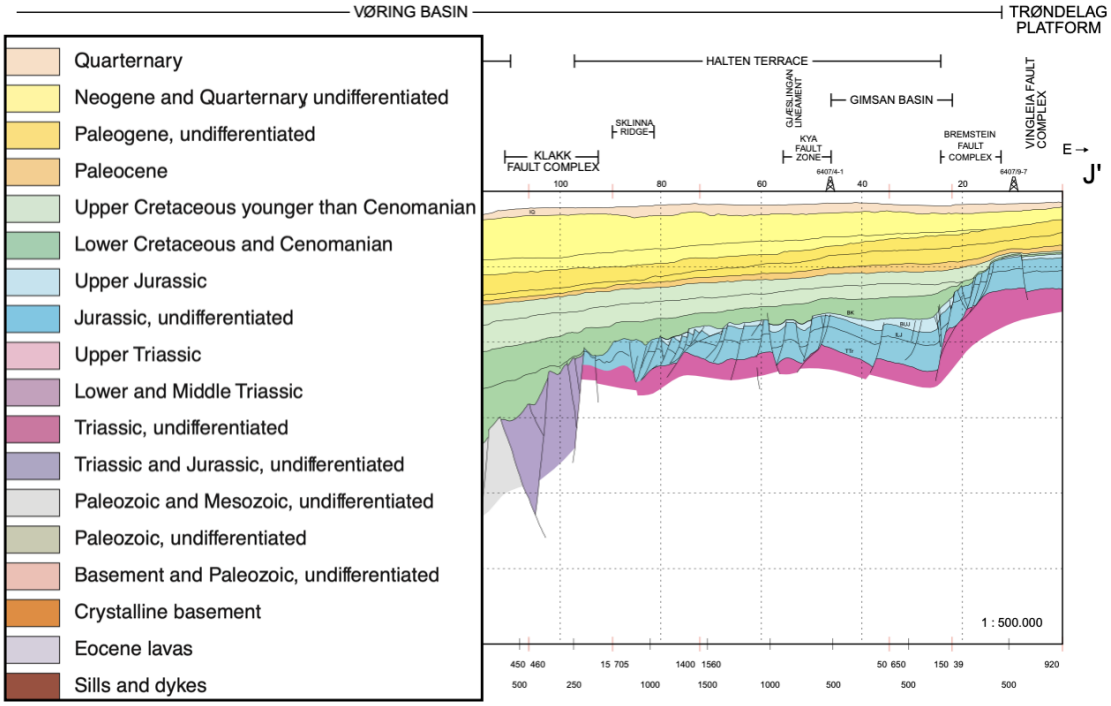

Figure 1.4: Halten Terrace stratigraphy. Modified from NPD Factpages.

Mid - Late Jurassic Rifting

The main rifting event in the study area is in the Jurassic (Lien, 2005). Prior to the Mid- Late Jurassic rift event, The Trøndelag platform and Halten Terrace were part of a relatively flat area, while the Froan Basin existed as a shallow sea (Færseth, 2021; Riis et al., 2014). The Vingleia fault complex, on the shallow part of the Halten Terrace in the Trøndelag platform area, and the Bremstein fault complex, separating the Halten Terrace in the east from the Trøndelag platform to the west, were initiated during the mid-late Jurassic rift event (Blystad et al., 1995). These fault complexes led to the Halten Terrace becoming a distinct structural entity (figure 1.4), down faulted in relation to the uplifted Trøndelag platform (Færseth, 2021; Riis et al., 2014). The Frøya High and the southwestern part of the Froan Basin also underwent uplift. An angular unconformity in the Froan Basin suggest uplift and deep erosion (Blystad et al., 1995).

Crustal thinning in the region is attributed primarily to the Jurassic rift events. Areas west of the study region, such as the Rås and Træna basins, experienced maximum thinning, which is evidenced by Cretaceous sediments overlying the basement. In the Rås Basin, extension caused thinning of the crust to less than 5 km and elevated the Moho (Færseth, 2021; Riis et al., 2014). As argued by (Nolan, 2021), heat flow estimates in this area are elevated, which is a result of crustal extension.

Post Jurassic rifting events

The transition from Late Jurassic to Early Cretaceous involved rifting, extension, and faulting, resulting in significant crustal thinning (Riis et al., 2014). Uplifted areas like the Frøya High underwent uplift and erosion, leaving the basement at shallower levels. Deep erosion areas experienced 1-2 km uplift in the footwalls of some of the largest faults (Færseth, 2021).

The Jurassic rifting triggered salt mobilization in Triassic evaporite deposits of the Halten Terrace, causing significant structures such as the Gimsan Basin on the southeastern part of the Halten Terrace. The formation of the Gimsan Basin resulted from the withdrawal of salt below the Base Cretaceous. While other structures of the Halten Terrace were influenced by salt mobilization, the Trøndelag platform experienced minimal impact from this (Færseth, 2021).

The base Cretaceous unconformity marks the transition from Jurassic rifting to post-rift thermal subsidence, potentially spanning tens of millions of years. The stratigraphy in the structural highs is complex, with Cretaceous sediments overlaying Jurassic structural highs due to a regional sea level rise.

The third rifting phase during the Cretaceous - Tertiary transition affected to a minor degree the area (Færseth, 2021). In the Tertiary, arctic seafloor spreading generated compression in the area, marking another change in stress regime in the geological his-

tory of the region (Riis et al., 2014). The previously thinned continental crust was uplifted and eroded (Færseth, 2021).

1.3.3 Stratigraphy

The study area exhibits heterogeneous lithology, with clastic rocks, primarily sandstone and shale, dominating the sedimentary sequence. However, distinctive properties within certain formations may influence the thermal regime. These properties include depth to basement, grain size, organic material, and volcanic tuffs. Despite indications in the literature suggesting the presence of evaporites, these were not encountered in the wells analyzed in this study. The lithostratigraphic column is presented in figure 1.5

Triassic

Triassic successions are classified as informal groups, characterized by 'grey beds' and 'red beds,' both of which are clastic, continental deposits. However, there was a notable climate shift during the mid to upper Triassic period, transitioning from a humid climate to an arid one. Consequently, red beds were deposited during the humid phase, followed by the accumulation of evaporite sequences. Subsequently, grey beds were deposited during the more arid climatic conditions. Both of these informal groups primarily consist of sandstones, although the uppermost intervals also contain significant shales and siltstones (NPD, 2023). Thick Triassic successions were deposited in the Froan Basin and other deep rift basins on the Trøndelag platform and Halten Terrace. Uplift and erosion led to the absence of Triassic deposits in many areas, so these locations are mainly the only places where the Triassic sediments are still present. Some areas may contain only lower or upper Triassic successions depending on the geological structure. Although uncertain, older successions could also be encountered, such as Early Triassic shales or Upper Permian carbonates (Færseth, 2021; Riis et al., 2014).

Jurassic

During the Early to Middle Jurassic, the Trøndelag platform and Halten Terrace experienced subsidence, leading to the infilling of basins with fluvial deltaic deposits. This resulted in the formation of a thick Jurassic succession on the Trøndelag platform, characterized by the presence of multiple aquifers. Below is a description of the Jurassic units (Riis et al., 2014).

Båt Group: Within the Båt Group, the Åre Formation is composed of sandstone, claystone, and coal interbeds, featuring vitreous coals that are locally pyritic. These sediments were deposited in a coastal to delta plain environment with swamps and channels. The Åre Formation is particularly significant due to the presence of coal, which makes it an important source rock.

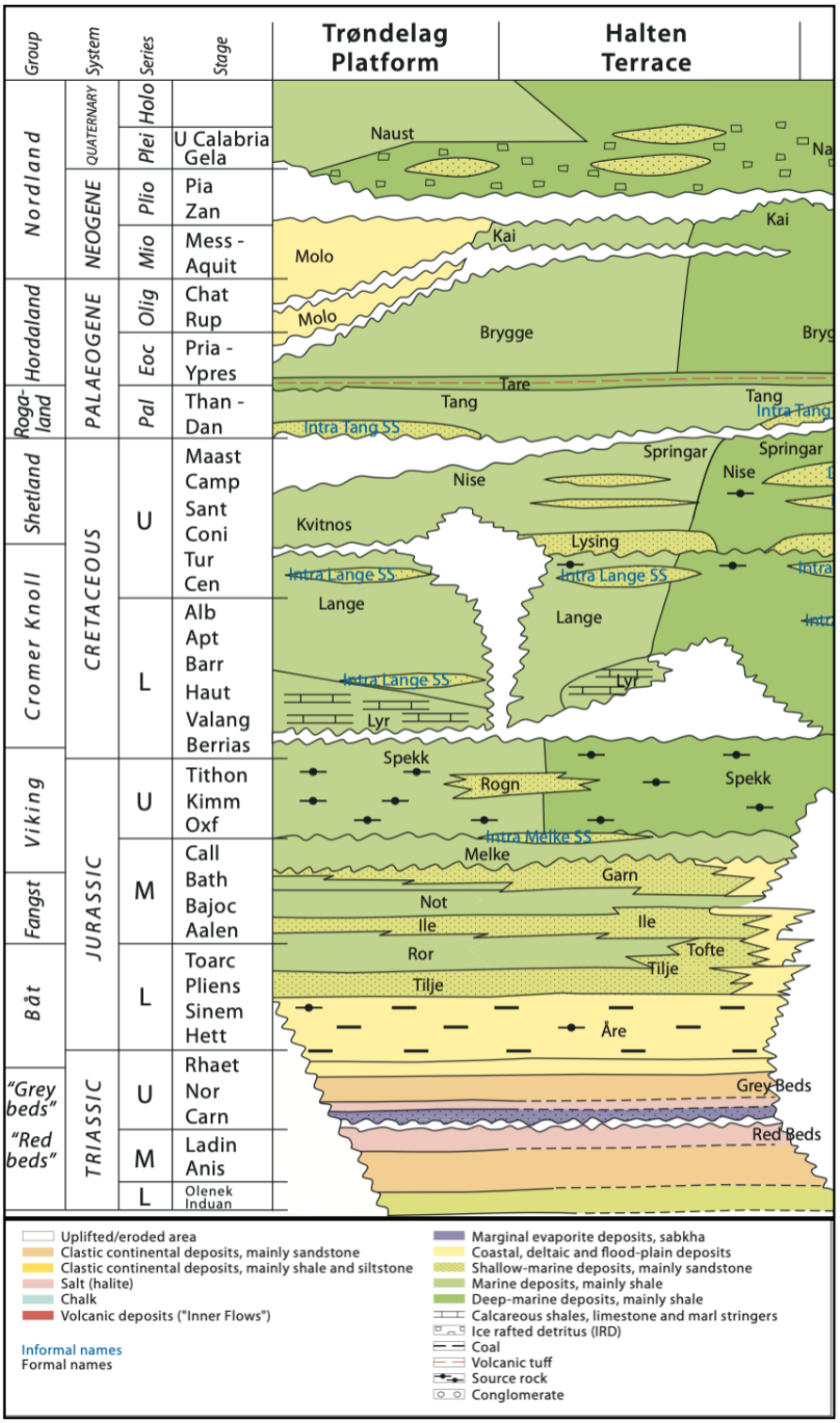

Figure 1.5: Stratigraphy of the Trøndelag Platform and Halten Terrace areas (NPD, 2023)

The Tilje Formation primarily consists of sandstones, accompanied by siltstone and shale interbeds. It exhibits bioturbated sandstones with inclusions of shale, coal, and peat clasts. This formation transitions from a marine to intertidal environment as it extends eastward into more continental settings.

The Ror Formation comprises mudstone with siltstone and sandstone interbeds, characterized by sandy and silty coarsening upward sequences. This formation reflects an open shelf environment, and variations in thickness are attributed to uplift along the western margins of the basin.

The Tofte Formation is predominantly composed of sandstones, with zones displaying very poor sorting and high clay content. It features coarse-grained, large cross-bedding, and the quartz content exceeds 90 %. The formation shows indications of uplift, as the deposits appear as fan deltas towards the east (Færseth, 2021). Notably, it should be acknowledged that the presence of coal within these formations can significantly impact thermal conductivity, with even a small percentage of coal causing a considerable reduction in the formation's conductivity (Evans & Coleman, 1974).

Fangst Group: The Fangst Group is characterized by sandstone and mudstone formations, comprising three formations deposited in various environments ranging from shallow marine and coastal settings to more continental ones. On the Halten Terrace, the Fangst Group displays characteristics of a shallow marine to coastal/deltaic environment, with an increasing continental influence in the lower formations.

The Ile Formation is predominantly dominated by mudstones, but in parts of the Trøndelag platform it has sandstones. These sequences consist of sandstones, siltstones, and shales interbeds, often featuring thin carbonate-cemented stringers in the lower sections and mica-rich intervals. These indicate a depositional setting of tidal deltas and coastlines.

The Not Formation is primarily identified by locally carbonate-cemented sandstones, claystones, and finer-grained sandstones interbedded with shaly material. Additionally, mica-rich, bioturbated sandstones and claystones with pyrite are notable components. It is important to mention that the Not Formation is predominantly shaly on the Trøndelag platform.

The lower section of the Garn Formation is the culmination of the sequence between the Permian-Triassic and Mid-Late Jurassic rift phases, while the upper section of the Garn Formation marks the initiation of the Mid-Jurassic rift phase. The Garn Formation is predominantly composed of sandstones, occasionally carbonate-cemented, and it

is characterized by mica-rich zones. It comprises a range of fine to coarse-grained sandstones, which are good reservoirs. The formation is a shallow marine deposit in most of the study area (Færseth, 2021; NPD, 2023).

Viking Group: The Viking Group represents a sedimentary sequence primarily deposited in a marine environment situated below the wave base. Consequently, the formations within this group are characterized by elevated clay content, with siltstone, shales, and mudstones being the dominant lithologies. In particular, the Melke Formation is noteworthy for its occasional occurrence of limestone interbeds; nevertheless, claystones remain the prevailing sediments, with certain sections displaying minor calcareous sediments.

The Spekk Formation within the Viking Group is distinguished by a substantial presence of organic content. Alongside the Åre Formation, it represents a significant Jurassic source rock, with the potential to have been the main hydrocarbon source in the region.

Conversely, the Rogn Formation exhibits a notably sandy composition and is frequently identified as a reservoir rock within the Halten Terrace. However, its reservoir potential is hindered in the Trøndelag platform due to shallower burial depths. (Dalland et al., 1998).

Cretaceous

In the Norwegian Sea, Cretaceous sediments are dominated by mudstones and siltstones (Riis et al., 2014).

Cromer Knoll Group Within the Cromer Knoll Group, specifically in the Lyr Formation, there is a higher concentration of carbonates, while the Lange Formation contains intermittent sandstone stringers but is primarily composed of claystones. The Lysing Formation is dominated by sandstones, with shale interbeds, and clastic sandstones are predominantly found in the upper part of the group. These sediments were deposited during the mid to late Cretaceous in the Norwegian Sea and are believed to represent the thermal subsidence stage following the Jurassic rifting event. The group could also be absent due to an unconformity. Notably, the Lyr Formation, exhibits variations in thickness and sedimentation rates (Færseth, 2021).

Shetland Group In the Shetland Group, minor amounts of carbonates are present, with claystones being the primary lithology across all three formations: The Springar, Nise, and Kvitnos. The claystones in the Kvitnos Formation are calcareous (Dalland et al., 1998). These formations were deposited in an open marine environment (NPD, 2023).

Tertiary

Rogaland Group The Rogaland Group includes the Tang and Tare formations, which are characterized by deep marine sediments, mainly claystone and minor siltstone and sandstone (Dalland et al., 1998). Seafloor spreading resulted in volcanic tuff deposits which are characteristic of the Tare Formation (Riis et al., 2014).

Hordaland and Nordland Groups The Nordland group is subdivided into the Kai, Molo and Naust formations. These formations primarily consist of claystones, siltstones, and sandstones. The group has glacial to glacio-marine origin in The Halten Terrace. Lower parts of the group have also glacial origin in the Trøndelag platform. The sandstones contain glauconite, pyrite, erratic sediments and shell fragments (NPD, 2023).

1.4 Background data

1.4.1 Temperature data

The initial temperature data utilized in this study involves a second-order polynomial fit applied to available temperatures, primarily from Drill Stem Test (DST) data. However, in cases where DST temperatures are unavailable, wireline Bottom Hole Temperature (BHT) measurements are employed as an alternative. A prerequisite for this estimation is the availability of temperature measurements in the lower 500 meters of the well. The uppermost data point, representing the sea floor, is standardized at 5°C. The BHT estimate is determined at the point of intersection between the polynomial fit and the well's depth profile (NPD, 2023).

Temperature measurements in deep boreholes, acquired post-drilling, are acknowledged to be impacted by the drilling process, primarily due to the cooling effect of mud circulation. Therefore, bottom-hole temperature (BHT) measurements may not accurately reflect the equilibrium temperature of the surrounding formation, depending on the timing of the measurement and the intended use of the data. Correction for time since circulation is necessary to obtain the equilibrium temperature of the formation (Hearst et al., 1988; Rider & Kennedy, 2014). DST temperatures still provide a more reliable estimate than corrected BHT values (Goutorbe et al., 2007) and do not require correction. Extrapolating these values should theoretically mitigate correction uncertainties.

1.4.2 Heat conduction in sedimentary basins

The subsurface is not homogeneous, and it is more reasonable to expect a non-linear gradient that takes into account the variations caused by differences in rock properties and structures. This can be done by considering a simple 1D model for heat conduction.

In the context of one-dimensional (1D) heat conduction, specific assumptions are employed. Firstly, the model assumes that heat is predominantly transferred through conduction, with convection and radiation contributing to heat flow but not considered as distinct parameters. The calculation of heat flow can be determined using equation (1.2). Secondly, the 1D model focuses solely on the vertical dimension of heat conduction. While exceptions exist, such as in regions with notably high thermal conductivity or specific tectonic settings, sedimentary basins generally experience upward heat movement, justifying the acceptance of this assumption (Kauerauf & Hantschel, 2009). This modeling approach allows for the identification of lower temperature gradients in layers with higher thermal conductivity, facilitating the estimation of thermal properties for each layer. A 1D model, based on the aforementioned assumptions and utilizing equation (1.3) for calculation (Fuchs et al., 2015), can be developed for given heat flow values.

$$T = T_0 + \sum_{i=z_0}^{z} \frac{q_i}{TC_i} \tag{1.3}$$

$$T = T_0 + \sum_{i=z_0}^{z} \frac{q}{TC_i} \tag{1.4}$$

Thirdly, this study assumes a constant heat flow. Modifying equation (1.3) yields a simplified 1D model, as expressed by equation (1.4). In sedimentary basins, radiogenic heat production from the crystalline basement contributes to the heat flow into the basin (Fuchs et al., 2015). Thus, the simplification of not including radiogenic heat could introduce errors (Kauerauf & Hantschel, 2009). The lack of heat flow data in the area, coupled with uncertainties in temperature data and thermal conductivity values, makes a steady-state heat flow assumption preferable for interpreting other parameters. Heat flow estimates provided by (Pascal, 2015) serve as a guiding reference. This author reports a heat flow value of 65 $\mathrm{mW/m^2}$ with a standard deviation of 7 $\mathrm{mW/m^2}$ on the Mid Norwegian Shelf. Despite being based on constant heat flow, these estimates, derived from various depths, indicate a vertical increase in heat flow with depth.

1.4.3 Thermal conductivity calculations

The complexity of thermal conductivity (TC) within rocks has led to the development of several approaches for its determination. While much of the comparable literature, such as (Pascal, 2015), has estimated the rock matrix thermal conductivity and subsequently considered additional rock properties that influence TC, (Fuchs et al., 2015) proposed

a statistical approach. This approach derives regression prediction equations for TC based directly on various well-log parameters, thus enabling a one-step determination where several properties are inherently reflected by the well-log responses. Furthermore, this method refines the estimation of TC in sedimentary rocks by accounting for the variability in porosity and its impact on the combined thermal properties of the mineral matrix and the fluids within the pores. This consideration is of particular importance in geological formations where porosity can significantly affect thermal behavior, such as in oil and gas exploration and geothermal gradient studies.

The prediction equations differentiate among synthetic 'rocks' that represent the three major rock types: clastics, carbonates, and evaporites. A distinct set of equations is provided for each rock type as outlined in Table 1.2. These equations utilize a combination of well-log responses, and multiple regression analysis is employed to predict TC with varying degrees of accuracy. For this thesis, the relevant equations for clastic rocks are detailed in equations (1.7) to (1.10), and carbonate rocks in equations (1.5) and (1.6). TC represents thermal conductivity, ΔT is the sonic interval transit time, ρ_b is the bulk density, Φ_N is the neutron porosity, and V_{sh} is the volume fraction of shale. The R^2 value denotes the coefficient of determination, indicating the prediction's degree of accuracy.

$$TC = 3.92 - 5.11\Phi_N, \quad R^2 = 59\% \tag{1.5}$$

$$TC = 5.84 - 0.0063\Delta T - 1.48V_{sh}, \quad R^2 = 77\% \tag{1.6}$$

$$TC = 3.41 - 4.83\Phi_N, \quad R^2 = 51\% \tag{1.7}$$

$$TC = 4.17 - 3.89\rho_b - 1.78V_{sh}, \quad R^2 = 76\% \tag{1.8}$$

$$TC = 3.66 - 5.13\Phi_N + 0.0029\Delta T - 1.70V_{sh}, \quad R^2 = 76\% \tag{1.9}$$

$$TC = -1.55 + 1.39\rho_b - 6.81\Phi_N + 0.0115\Delta T - 1.53V_{sh}, \quad R^2 = 79\% \tag{1.10}$$

Geophysical well logs

Four types of well logs were used in this thesis. The Gamma Ray (GR) log, the Neutron Porosity log, the Sonic log, and the Density log.

The Gamma Ray (GR) log identifies natural radiation from Uranium, Thorium, and Potassium in a geological formation. Due to its ability to detect elevated radiation levels in shales, the GR log is commonly referred to as a 'shale log.' The data obtained

Mineral	Carbonates (%)	Clastic rocks (%)	Evaporites (%)
Quartz	0–50	50–100	-
Anorthite	-	0–50	-
Albite	-	0–50	-
Orthoclase	-	0–50	-
Muscovite	-	0–20	-
Biotite	-	0–20	-
Kaolinite	0–70	-	-
Montmorillonite	0–70	0–100	-
Illite	0–70	0–100	-
Calcite	0–100	0–20	0–100
Dolomite	0–100	0–20	0–100
Anhydrite	-	0–20	0–100
Gypsum	-	-	0–100
Halite	-	-	0–100
Sylvite	-	-	0–100

Table 1.2: Sedimentary rock groups based on assumed composition and mineral content ranges. Source: Fuchs et al. (2015)

from the GR log is valuable for calculating shale volume using equation (1.11) (Rider & Kennedy, 2014).

$$Vsh[\ \%] = \frac{GR - GR_{min}}{GR_{max} - GR_{min}} \cdot 100\% \tag{1.11}$$

The Neutron Porosity log provides information about the hydrogen content, primarily indicating the water content within a geological formation. In practical terms, it offers an estimate of the formation's porosity. In the context of TC determination, porosity logs are important because they allow for the prediction of bulk TC of the rock, not only the matrix TC (Fuchs et al., 2015).

The Sonic log measures the slowness of a formation by recording the time it takes for a sound pulse to traverse a known distance through the formation. The reciprocal of this travel time gives the sonic velocity.

Density log measures bulk density, which represents the density of the mineral composition and fluids within a rock. (Rider & Kennedy, 2014).

Furthermore, the density and sonic logs can be employed to estimate acoustic impedance, a property that characterizes the resistance of a material to the propagation of sound waves. This parameter is useful for distinguishing carbonates from clastic rocks (Mello & Lupinacci, 2022).

Method

2.1 Data acquisiton

The study area featured a total of 80 wells from which data could potentially be retrieved. NPD´s Factpages served as the primary resource for identifying available data. Initially, emphasis was placed on the search for well log data, given its essential role in thermal conductivity calculations. Notably, a limited number of wells contained a photoelectric factor log, leading to the decision to exclude this log from the calculations despite the awareness that such exclusion could result in more uncertainties.

To streamline the data acquisition process, a selection process was undertaken to avoid exporting unnecessary information. Only wells housing fundamental geophysical well logs, including density, gamma ray, sonic, and neutron porosity, were considered. These wells were obtained as LAS files from DecisionSpace and Diskos. A thorough quality check was implemented to verify the presence of all essential logs within the same depth intervals. While most wells lacked comprehensive data across all depths, the criterion for inclusion rested on the availability of all required data within specific depth intervals, ensuring the possibility of thermal conductivity calculations at those intervals.

Subsequently, for the following steps, the identification of bottom hole temperatures was considered necessary. Factpages was revisited to extract this data, revealing that certain wells lacked this information. Some wells featured specific bottom hole temperature measurements, with details about *time since circulation* often absent, while most wells had bottom hole temperature estimates based on linear interpolation from measurements. As a result, a decision was made to only include wells where this data was determined through linear interpolation so that the potential errors would be of similar degree across all wells.

Finally, additional relevant data, such as depth measurements, coordinates, and lithology, was extracted from factpages. Upon the completion of the data acquisition phase, a subset of 42 wells remained for further analysis.

2.2 Linear gradient

Utilizing equation (1.1) alongside temperature and depth data obtained from the Norwegian Petroleum Directorate (NPD), linear temperature gradients were calculated for individual wells. These gradients enabled comparisons to the estimated geothermal gradient and were used as initial temperature values for intervals with absent data.

2.3 Classification of rock units

To compute TC using the equations outlined in (Fuchs et al., 2015), the initial step involved categorizing depth intervals within the well as either clastics, evaporites, or carbonates. The LAS files were imported into Petrel, where a manual classification was conducted. The classification was based on the well logs available, which were often more logs than the required logs for the TC calculations. The well log responses were initially interpreted alongside completion reports and general lithological information from NPD. The classification was only performed in the depth intervals where all necessary logs were available.

Due to the heterogeneity in the formations, the results of the manual interpretation seemed unreliable. To address this issue, an algorithm was employed for rock type classification, developed by identifying a distinctive carbonate interval where carbonate content was clearly defined in well log responses. Acoustic impedance and gamma ray responses at this interval served as a guideline, with initial criteria set to an acoustic impedance value $> 10{,}000$ and a gamma ray value < 25 API.

Further refinement of the algorithm was necessary due to the recurring pattern of calcareous shales and marls in various formations. The gamma ray value threshold was adjusted to GR < 35 to accommodate these lithologies. Consequently, sections with an acoustic impedance $> 10{,}000$ and gamma ray < 35 were classified as carbonates, while the remaining sections were designated as clastics, as evaporites was not considered.

The algorithm was systematically applied to all depth intervals containing essential logs for classification. Within the files, newly established well sections were designated with rock type classifications, where each rock type was represented by a number in the LAS files.

2.4 Thermal conductivity calculation

To compute thermal conductivity, the volume of shale log was necessary. Thus, the volume of shale was calculated using Petrel by applying equation (1.11) to the gamma ray log at each depth step, and the resultant values were assigned to a newly created well section.

Following this, the resulting well sections were exported from Petrel as LAS files. The rock type section, serving as the exported depth interval, ensured the exclusion of depths lacking sonic, gamma ray, and density log data. This methodology preemptively mitigated the need for future data cleaning. These files formed the the basis for subsequent thermal conductivity calculations.

To calculate thermal conductivity for carbonates and clastics, equations (1.6) and (1.9) were selected due to their minimal uncertainties given our data coverage. Using the new LAS files and a function that assigned the appropriate equation based on rock type classification, the calculations were initially executed in Python. The TC values were plotted against depth to assess the results.

Unexpectedly, the plots revealed negative values, prompting another data quality check. Examination of the log data in Petrel uncovered neutron porosity logs represented in percentage form rather than as fractions, which was the form required in the calculations. This issue was resolved within Petrel, and one file was exported to reassess the results using the functions in Python. While this correction partly resolved the issue, many wells still remained unreasonable.

Due to anomalies and the availability of multiple equations in (Fuchs et al., 2015), alternative equations were considered despite the elevated uncertainties related to these other equations. Implementing other equations directly into Petrel provided a comprehensive analysis, allowing for the testing of multiple equations to assess the outcomes, without needing to export and import all the files between each test. The best fit equations (1.6) and (1.9) were roughly quality checked in Petrel, and then exported for a more detailed quality check in Python. TC histograms for each well were created, which confirmed that the data was reasonable, but in order to further investigate these values, histograms of TC were also created for each formation, these value ranges were also plotted against depth, to be able to compare values within the formations and take depths into account - as this can also affect the values.

2.5 Geotherml Gradient

The initial approach to reconstructing the thermal gradient was to utilize a linear gradient, following the methodology outlined in equation (1.1). This step served as a basis for comparison and was particularly useful due to the scarcity of data. Initial temperatures derived from this gradient were subsequently applied in the reconstruction of the geothermal gradient. The geothermal gradient was calculated using the equation (1.4), setting the heat flow to 65 mW/m^2, based on estimates from Pascal (2015).

In the refined approach for estimating subsurface temperatures, a brute-force grid search method was utilized, offering more flexibility than assuming constant heat flow for each well. First, the thermal conductivity (TC) values were filtered to exclude outliers. Sub-

sequently, a grid combining potential TC values for intervals with missing data and a range of heat flow (q) values was established. The objective was to identify the TC and q combination most accurately aligning with the observed bottom-hole temperature (BHT). Boundary limits for TC were defined as the maximum and minimum values in each respective well, while the default range for q was set between 55 and 75 m/Wm^2, reflecting typical estimates. The estimation of subsurface temperature and thermal gradients involved a systematic exploration of every q and TC combination within these predefined ranges and at reasonable intervals. 'Guess' values for q and TC were initially used, and the 'best' values were determined as those minimizing the misfit in BHT, which represents the discrepancy between the reported BHT and the model-estimated BHT. Key geological formations within each well log were identified, enabling the computation of mean TC values for each formation. These mean TC values were then compared against the filtered TC log. Depth intervals corresponding to each formation were color-coded based on geological age, providing a visual context for the resulting plots.

Results

3.1 Data Acquisition

The study area features a total of 80 wells from which data could potentially be retrieved. Upon completion of the data acquisition phase, a subset of 42 wells was selected for further analysis.

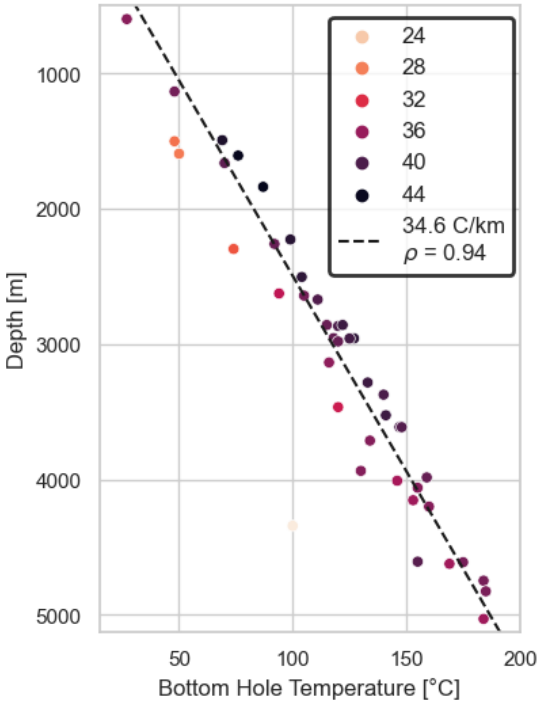

Figure 3.1: Plot based on data from NPD FactPages showing linear estimations of bottom hole temperature.

A plot of BHT versus depth is presented in figure 3.1. The average bottom hole temperature (BHT) of all wells is 119.4 °C. Based on the depth and BHTs, the average geothermal gradient for all wells is 34.6°C/km. These measurements provide insight

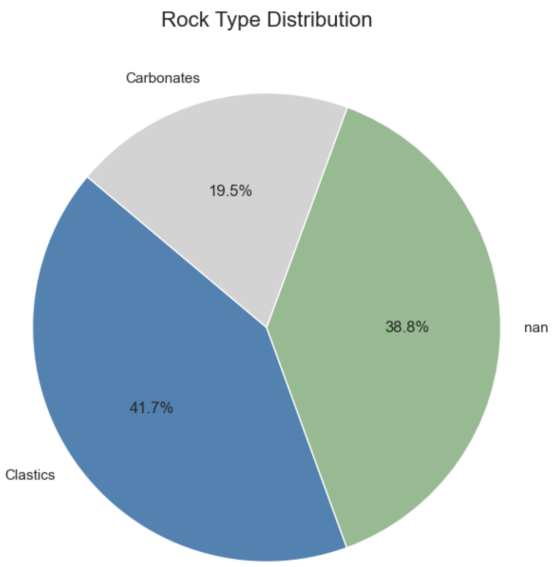

Figure 3.2: Proportion of clastics, carbonates and missing data in study area.

into the thermal regime and reflect the expected increase of temperature with depth. It is important to note that BHTs varied significantly across different wells, making the average gradient not fullly representative of the entire study area.

3.2 Rock Type Classification

Examination of geological reports identified clastic rocks as the predominant type within the study area. However, the reports indicated an ambiguous definition of carbonate content. Thick carbonate intervals were infrequent; instead, carbonates often appeared as limestone and dolomite stringers, carbonates partially cemented, calcareous shales, and marls. Consequently, relying on manual lithological interpretation based on well logs introduced considerable uncertainty. The geological reports indicated a predominance of clastic rocks in the area, with no significant presence of evaporites. Following these guidelines and applying the classification algorithms, the resulting proportions of clastic and carbonate formations are illustrated in figure 3.2.

3.3 Thermal conductivity

To calculate thermal conductivity for carbonates and clastics, equations (1.6) and (1.10) were initially selected due to their minimal uncertainties given our data coverage. Negative values stemmed from equation (1.10), and these of course are incorrect. After testing several equations, equations (1.6) and (1.9) seemed most reliable based on the degree of accuracy in the calculation and the obtained value ranges.

3.3.1 Distribution of thermal conductivity by formation

Although the data from most wells and formations are widely scattered, it is possible to recognize some patterns. As displayed in figure 3.3, the distribution of thermal conductivity is more variable for the Jurassic formations, potentially due to the rifting events that influenced the area during that period. Additionally, the thermal properties of Jurassic source rocks and reservoir rocks may have affected the thermal regime. To identify specific patterns, a more detailed investigation of the groups and formations is necessary.

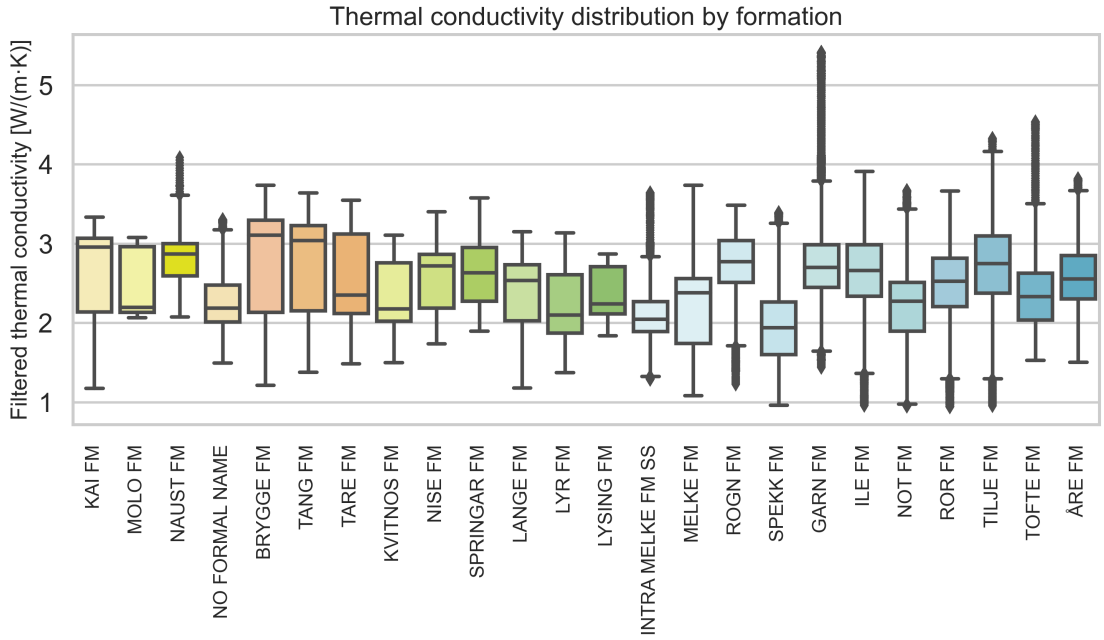

Figure 3.3: Thermal conductivity distribution by formation. Each box represents the interquartile range (IQR) of thermal conductivity values for a formation, with the horizontal line indicating the median. The whiskers extend to the furthest data point within 1.5 times the IQR from the box, and outliers are represented as individual points beyond the whiskers.

Båt Group

The mean thermal conductivity values for the formations within the Båt Group range from 2.4 to 2.7 W/mK, and figure 3.4 presents the distribution of thermal conductivity for each formation across all wells.

The thermal conductivity distribution for the Åre Formation is unexpectedly uniform, despite the presence of coal and sandstone, which typically exhibit significantly different conductivities. The presence of coal, even in small quantities, can markedly reduce thermal conductivity due to its much lower thermal conductivity relative to typical reservoir

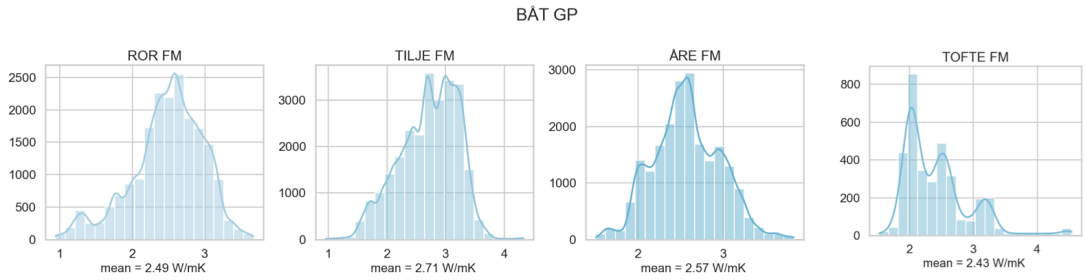

Figure 3.4: Histograms showing the distribution of thermal conductivity values within relevant formations of the Båt Group. Each histogram provides a frequency count of thermal conductivity values, with the mean conductivity annotated.

rocks. One might expect this to either result in an uneven distribution or significantly lower the mean value. However, the global values do not reflect this, suggesting a minimal presence of coal. Additionally, the influence of coastal deposits may enhance conductivity.

The Tofte Formation initially had a notable proportion of values exceeding 5 W/mK, which were reduced after data filtering. The elevated thermal conductivity values could be attributed to the high quartz content within the sandstones. Nonetheless, the heterogeneity of the formation—characterized by high clay content, poor sorting, and coarse grains—could attenuate conductivity. Furthermore, as depicted in figure 3.4 and the lithostratigraphic column, the formation does not appear frequently within the area, suggesting that the specific composition of the successions present may not represent the bulk lithology of the formation. A frequency count also indicated a limited number of data points or layers for this formation within the study area.

The mean thermal conductivity of the Tilje Formation is among the highest within the group, with a uniform distribution but a slight increase in frequency at higher values. The dominance of sand in the formation typically results in higher thermal conductivity due to better particle packing and mineral composition when compared to formations like shales. There could be lower thermal conductivity values in wells towards the east, attributable to changes in the depositional environment. This is illustrated in figure 3.5. Infrequent lower values may be associated with coal, peat, or shale clasts.

The Ror Formation exhibits heterogeneous lithology, primarily composed of mudstone, siltstone, and sandstone, without extremes in thermal conductivity values. The distribution of TC is within expected ranges, except for some outlier values on the lower end. These outliers could be indicative of a higher clay content, assuming clay is not prevalent within the area. Additionally, coarsening of the formation upward may impact the geothermal gradient.

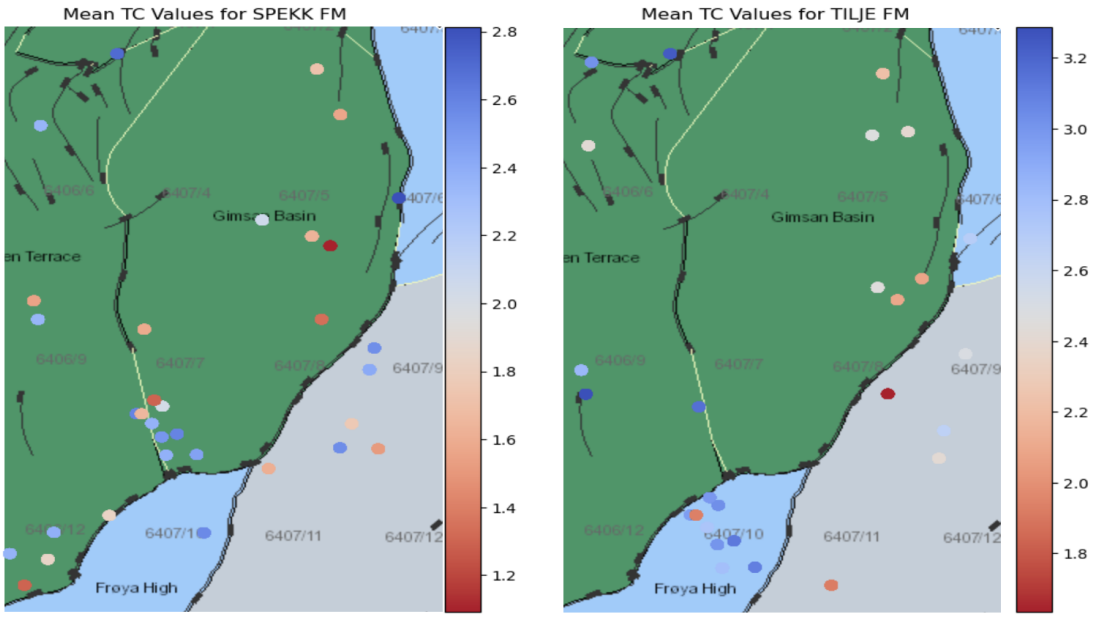

Figure 3.5: Spatial distribution of mean thermal conductivity (TC) values within the Spekk and Tile formations. The mean TC values for Spekk Formation seem to be relatively higher in the southern part of the displayed area, near the Frøya High, and tend to decrease towards the north and east, closer to the Gimsan Basin. In contrast, in the Tilje Formation, the mean TC values are generally higher than in the Spekk Formation, likely due to higher organic content in the Spekk Formation. The TC of the Tilje Formation also decreases towards the northern and eastern parts of the area.

Fangst Group

The Fangst Group exhibits lower thermal conductivity values in the Not Formation, consistent with its lithological characteristics, which include a high clay content (figure 3.6). The mean thermal conductivity of the Not Formation is 2.24 W/mK, marking it as one of the lowest among all formations in the study area. Although there are outliers, these typically present even lower conductivity values.

The Ile Formation displays significantly higher TC values, likely attributed to its increased sand content relative to the Not Formation. The distribution of TC values is broad, with many data points ranging between 2 and 3.5 W/mK.

The Garn Formation possesses even higher mean TC values at 2.87 W/mK. The distribution of values is relatively concentrated around the mean, with some outliers extending up to 5 W/mK. Given its stratigraphic significance, a more detailed investigation of the Garn formation by depth could yield insightful results.

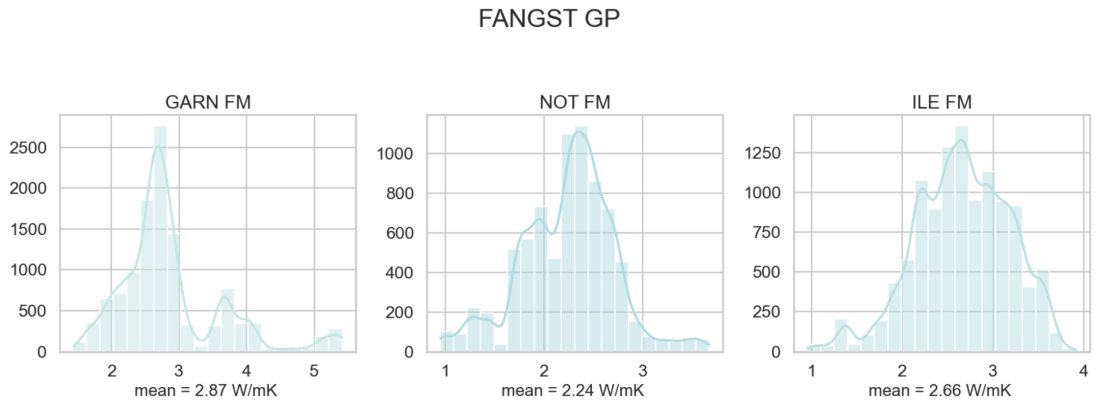

Figure 3.6: Histograms showing the distribution of thermal conductivity values within relevant formations of the Fangst Group. Each histogram provides a frequency count of thermal conductivity values, with the mean conductivity annotated.

Viking Group

The Viking Group, characterized by its elevated clay content, generally shows lower thermal conductivity values (figure 3.7). Nonetheless, the thermal conductivity can vary considerably depending on the presence of fluids within the rock matrix, whether organic or saline in nature.

The Spekk formation, with a mean TC of 1.96 W/mK, exhibits the lowest thermal conductivity of all formations examined, which can be primarily ascribed to its high organic content. The geographical distribution of TC values in this formation is given in figure 3.5, and it resembles that of the Tilje Formation, with TC decreasing to the

north and east.

The Melke Formation displays heterogeneous thermal conductivity values. It is worth noting that there may be confusion in some wells between the Melke formation and the Intra Melke formation Sandstone (SS), with the latter being sandier and, consequently, associated with higher TC values.

In the Rogn Formation, the most frequent TC values are observed above the mean of 2.75 W/mK. Being a sandstone formation, the observed range of TC values is within the expected parameters.

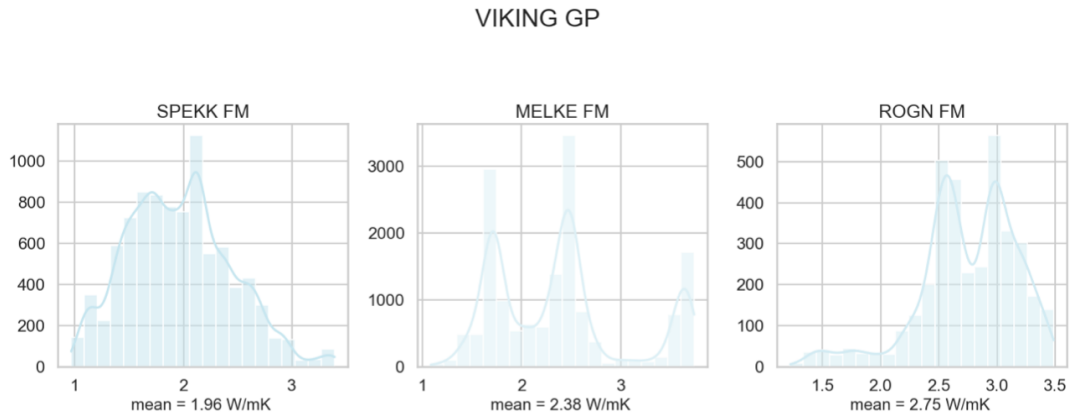

Figure 3.7: Histograms showing the distribution of thermal conductivity values within relevant formations of the Viking Group. Each histogram provides a frequency count of thermal conductivity values, with the mean conductivity annotated.

Cromer Knoll Group

In the Cretaceous Cromer Knoll Group, the thermal conductivity values as depicted by histograms appear more uniform than those in the Jurassic formations, suggesting a more consistent thermal regime (figure 3.8). The average thermal conductivity for the group at each well is given in figure 3.9.

The Lange Formation displays a significant TC range, with most values between 2.5 and 3 W/mK and some lower values reaching down to 1.5 W/mK (figure 3.8). The highest frequency is at 2.75 W/mK, followed by a lower peak at 2.0 W/mK, and the lowest peak at 1.6 W/mK. The mean TC value of 2.39 W/mK is not representative of this distribution. The frequency peaks likely correspond to variations between sandstone stringers and claystone within the formation.

The Lysing formation shows two pronounced peaks at approximately 2.2 and 2.7 W/mK, making the mean value of 2.38 W/mK non-representative of the formation's bimodal

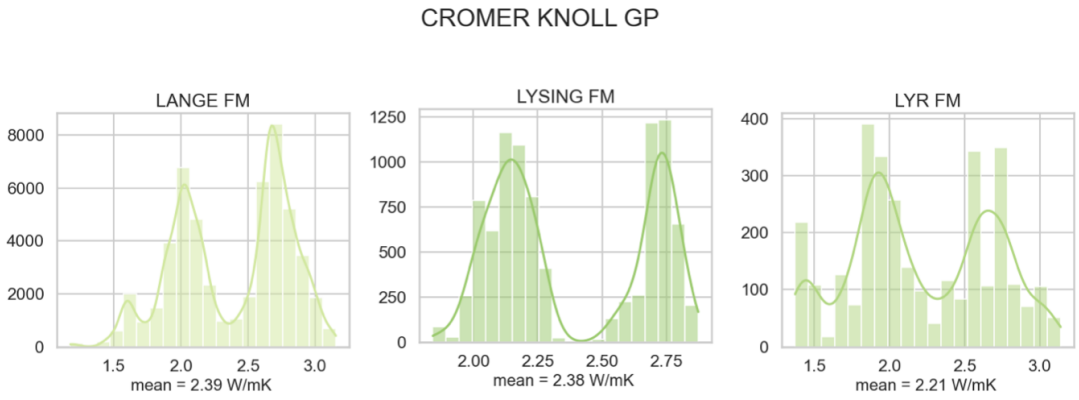

Figure 3.8: Histograms illustrating the distribution of thermal conductivity within the Lange and Lysing formations of the Cromer Knoll Group. Each histogram provides a frequency count of thermal conductivity values, with the mean conductivity annotated.

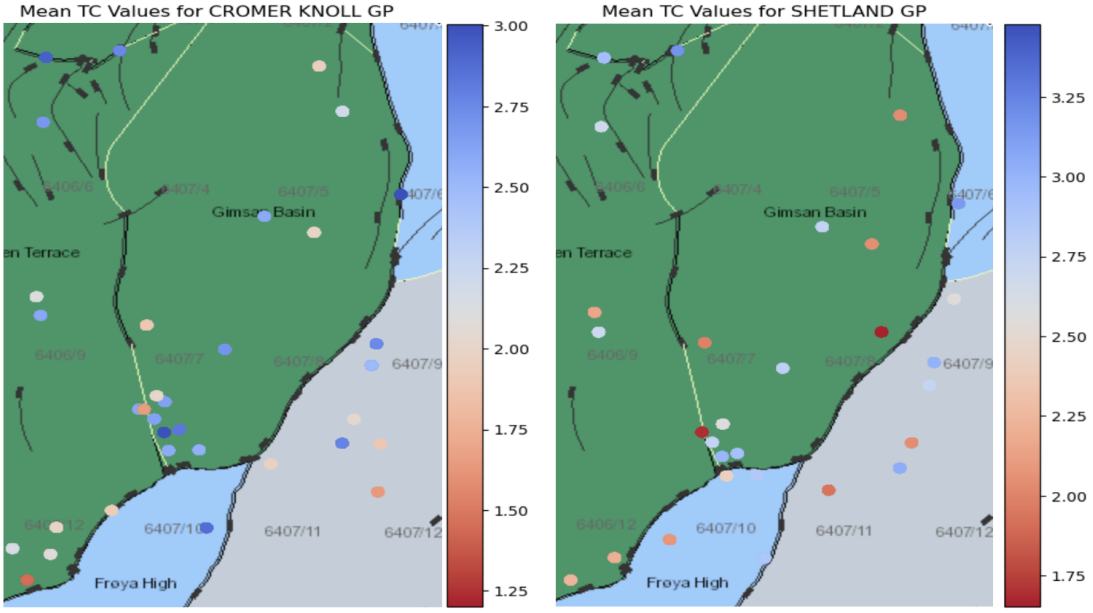

Figure 3.9: Spatial distribution of mean thermal conductivity (TC) values within the Cromer Knoll Group and the Shetland Group. In the Cromer Knoll Group, a broader range of TC values is observed, with higher values concentrated near the southern part of Gimsan basin and Grinda Graben, and lower values towards the Frøya High/ Halten Terrace boundary in the south. In contrast, the Shetland group exhibits a more uniform distribution of lower TC values, and this reflects a more homogenous lithology between the formations of the group.

distribution. This could indicate distinct thermal properties of the shale and sandstone sequences, or a contrast between the upper and lower sequences, as clastic sandstones predominate in the upper part of the formation.

The Lyr formation is not present much in the area due to the base Cretaceous unconformity. This formation displays a broad range of values from 1.5 to 3.0 W/mK. Given the low number of samples, the mean value of 2.21 W/mK does not represent the formation's thermal conductivity.

Shetland Group

Formations within the Shetland Group predominantly comprise shale and clay, although the Kvitnos Formation is more calcareous and has distinctly lower thermal conductivity compared to the other formations in the group (figure 3.10). Importantly, both the Nise and Kvitnos Formations exhibit dual peaks in their thermal conductivity distributions. However, the geographical distribution of TC shown in figure 3.9 considers only the average TC of the group and does not account for these dual peaks, resulting in relatively uniform TC distribution.

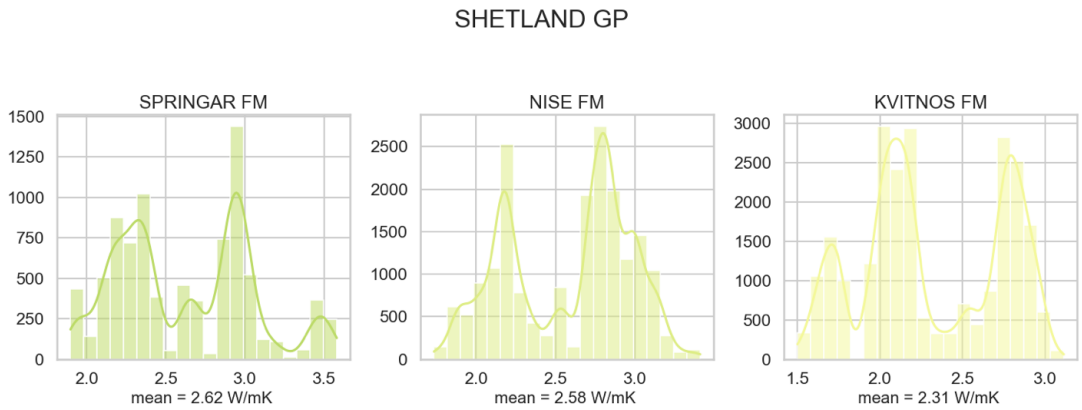

Figure 3.10: Histograms displaying the thermal conductivity distributions for the Nise and Kvitnos Formations of the Shetland Group, with dual peaks indicative of lithological variations.

Rogaland Group

Contrary to expectations based on the presence of volcanic tuff in the Tare Formation, thermal conductivity values were not elevated in this formation (figure 3.11). In fact, the Tang Formation exhibits higher TC values than the Tare Formation. This discrepancy may stem from a lack of tuff in many sampled wells or possibly the inadequacy of the thermal conductivity equation to account for the tuff's properties.

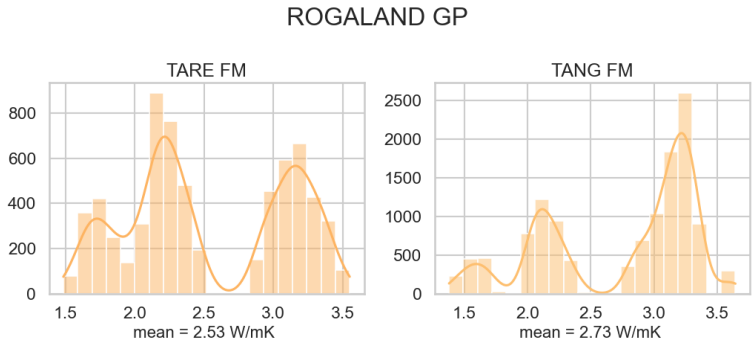

Figure 3.11: Histograms comparing the thermal conductivity of the Tang and Tare Formations in the Rogaland Group, highlighting the unexpected lower values in the Tare Formation despite its tuff content.

Hordaland Group

The Brygge Formation in the Hordaland Group exhibits a high frequency of occurrences, with a pronounced peak at approximately 3.4 W/mK (figure 3.12). This peak, along with frequently occurring values around 2.1 W/mK, may relate to the westward transition of the formation to deeper marine depositional environments.

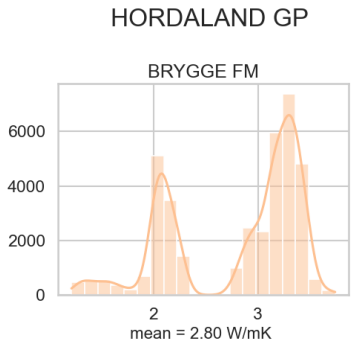

Figure 3.12: Histograms showing the thermal conductivity distribution of the Brygge Formation in the Nordland Group, with the prominent frequency peaks.

Nordland Group

The Naust Formation is characterized by relatively homogeneous and high thermal conductivity, with a mean of 2.8 W/mK (figure 3.13). The incorporation of ice-rafted detritus may enhance thermal conductivity, reflecting the influence of paleoclimate. The Kai Formation also exhibits homogeneity in TC, primarily around 3.0 W/mK, with a significant count at 2.1 W/mK. Depositional environmental changes towards deeper marine conditions in the west could influence conductivity through factors such as increased saltwater or more fine-grained materials. The Molo Formation exhibits a larger

concentration of TC values around 2.0, and a smalle one at around 3.0 W/mK.

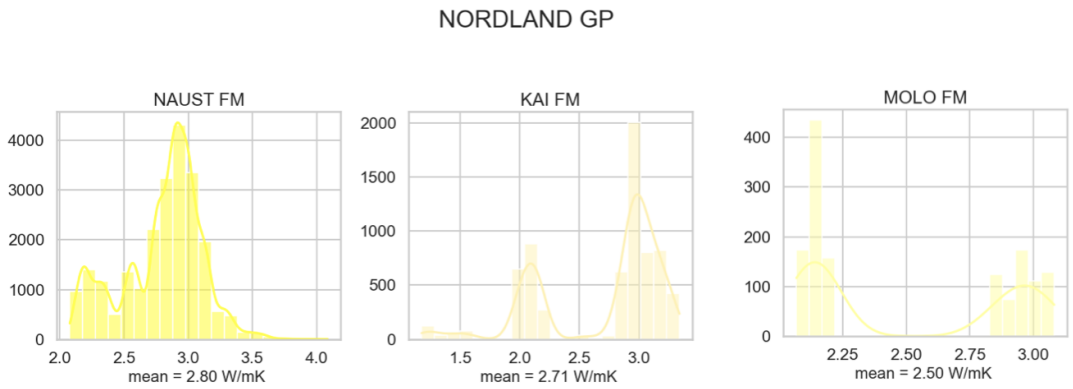

Figure 3.13: Histograms showing the thermal conductivity distribution of the Naust, Kai, and Molo Formations in the Norland Group. Gray histogram is for point data where formations were not identified.

In summary, the most significant formations are those where thermal conductivity values occur with high frequency, as low occurrence or lack of data affects all wells equally. However, using a mean TC value in formations exhibiting a wide range of thermal conductivty values due to heterogeneities or uncertainties may bias the analysis and results.

3.4 Geothermal Gradients

Due to the large amount of wells and the complexity of the study area, the resulting geothermal gradients are categorized by considering both the geological provinces and the actual well locations. This classification facilitates an interpretation that considers structural setting and other location factors. It further allows for the correlation between wells that exhibit similar characteristics. The study area is divided into five sub-areas: the Western Halten Terrace, the Northern Trøndelag Platform and Northeastern Gimsan Basin, the Southeastern Gimsan Basin, the Southwestern Halten Terrace and Frøya High, and the Froan Basin (figure 3.9).

3.4.1 Western Halten Terrace – Central West and Northwest, including the Grinda Graben

The wells in these areas are relatively deep, typically 4-5 km. A common trend observed is a continuous decrease in thermal conductivity within the Cretaceous strata, which aligns with the data from this region, as shown in figure 3.9. In the central area of the Gimsan Basin, thermal conductivity values tend to be below the global mean values, whereas higher values are observed in the central part of the Grinda Graben Table 3.1 and figures 3.14 to 3.16.

Well Name	Linear Gradient (°C/km)	Location
6407/1-3	35.6	NW, Grinda Graben
6406/3-2	36.9	NW, Grinda Graben
6407/1-1	36.8	NW
6406/3-1	35.5	NW
6406/6-6	37.6	Central W
6407/4-2	38.6	Central W, Gimsan Basin
6406/9-2	35.6	Central W
6406/9-1	37.7	Central W
6407/7-8	37.5	Central W, Gimsan Basin

Table 3.1: Geothermal gradients of wells in the Western Halten Terrace, including the Grinda Graben in the north. The northwestern wells are located just south of the Grinda Graben. The central wells of the Halten Terrace border the Gimsan Basin to the east, with some wells situated on the western flank of the Gimsan Basin.

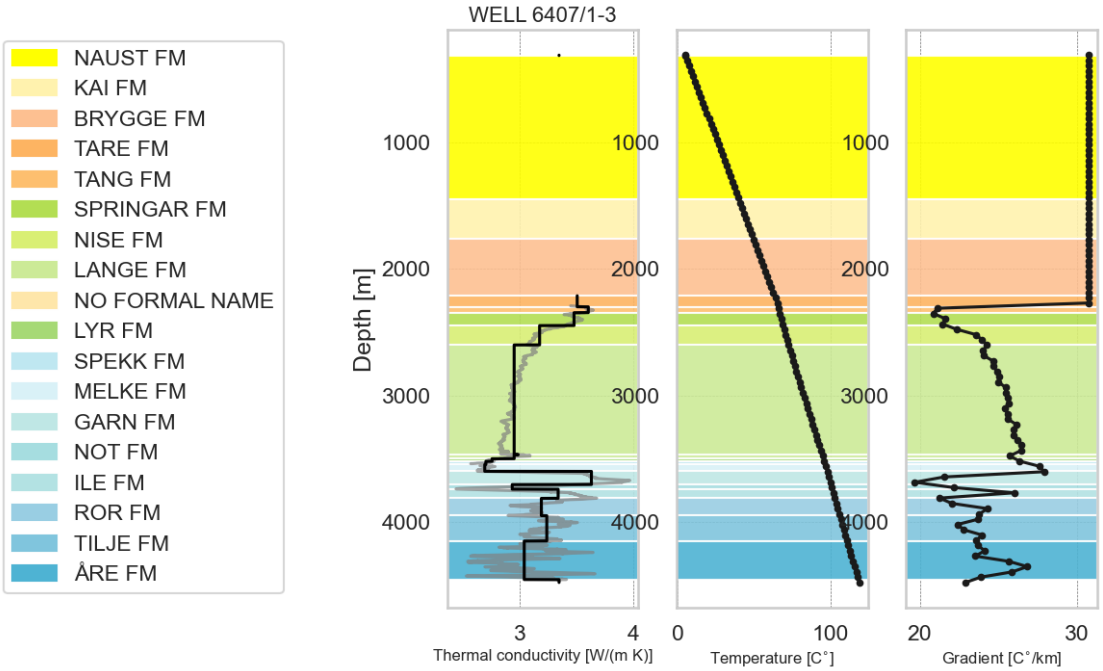

Figure 3.14: Thermal conductivity, temperature, and geothermal gradient versus depth for well 6407/1-3. The heat flow (q) ranges from 55 to 75 mW/m^2, and the estimated q value is 75 mW/m^2. The thermal conductivity above the data points (TC) ranges from 2.4 to 4.0 W/mK, and the estimated value is 2.4 W/mK. The measured Bottom Hole Temperature (BHT) is 153°C, whereas the estimated BHT is 118.8°C. The misfit in BHT values is -34.2°C, suggesting potential deviations from the assumed conditions or data inaccuracies. A total of 357 TC and q combinations were tested.

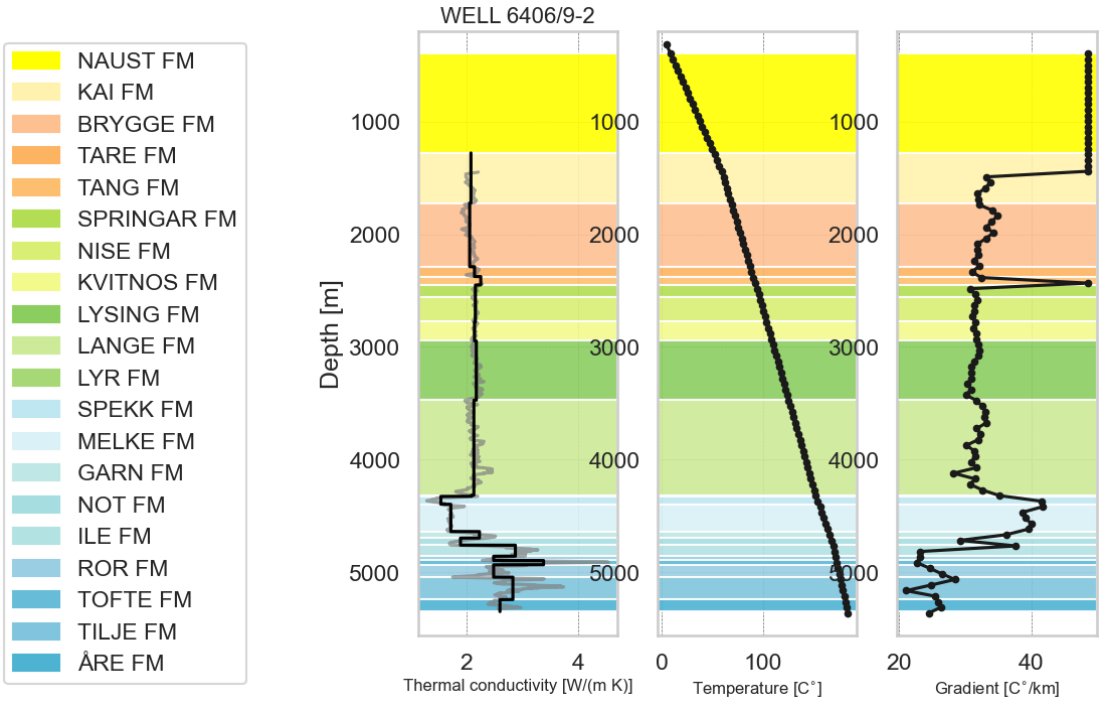

Figure 3.15: Thermal conductivity, temperature, and geothermal gradient versus depth for well 6406/9-2. The heat flow (q) ranges from 55 to 75 mW/m^2, and the estimated q value is 68 mW/m^2. The thermal conductivity above the data points (TC) ranges from 1.3 to 4.6 W/mK, and the estimated value is 1.4 W/mK. The measured Bottom Hole Temperature (BHT) is 184°C, and the estimated BHT is the same. A total of 714 TC and q combinations were tested.

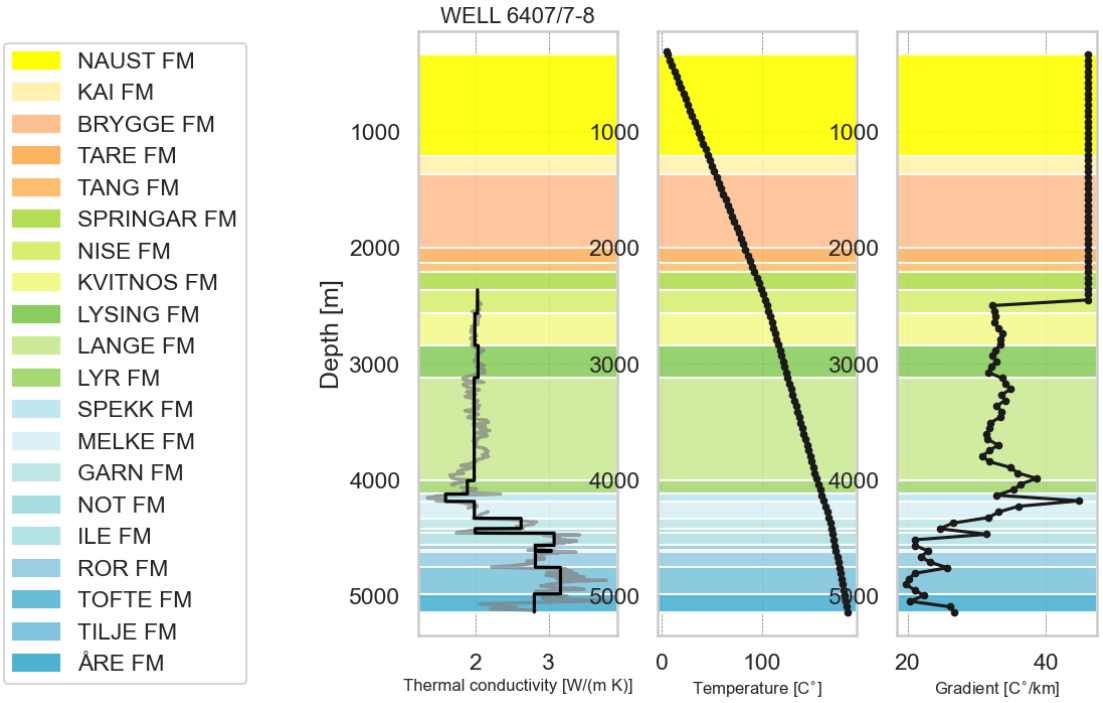

Figure 3.16: Thermal conductivity, temperature, and geothermal gradient versus depth for well 6407/7-8. The heat flow (q) ranges from 55 to 75 mW/m^2, and the estimated q value is 66 mW/m^2. The thermal conductivity above the data points (TC) ranges from 1.3 to 4.8 W/mK, and the estimated value is 1.4 W/mK. The measured Bottom Hole Temperature (BHT) is 185°C, and the estimated BHT is almost the same 185.5°C. A total of 546 TC and q combinations were tested.

Jurassic sediments exhibit significant variations in TC and thermal gradient, with clear variations both between and within formations. Only the Spekk Formation and Melke Formation of the Viking Group are consistently present in this part of the study area, while most wells include all formations from the Fangst Group. In the Båt Group, the formations present vary, and the sequence does not adhere to the typical stratigraphic order from oldest to youngest going upwards. This suggests structural complexity within the area.

In the Tertiary, data are generally sparse. Nonetheless, a trend of lower thermal conductivity values in the Tare Formation compared to the Tang Formation aligns with the broader global distribution. It is important to note that the peak in the gradient at the base of Rogaland group in well 6406/9-2 (figure 3.15), is an artifact from missing data, and not a drop in TC. The Nordland and Hordaland Groups display thicknesses similar to wells in other areas. None of the wells in this area indicate the presence of the Molo Formation. All other formations are present, with the exception of well 6407/1-1, which is notably shallow and exclusively drilled into the Naust Formation, and well 6406/3-2, which lacks data for the Naust Formation. Only one well in this area, well 6406/3-1 (located northwest on the Halten Terrace, south of the Grinda Graben), provides thermal conductivity data for these groups. This well exhibits thermal conductivity values for the Naust Formation ranging from 2.5 to 3.0 W/mK, but there is a noticeable and abrupt increase from 2.5 to 3.0 W/mK at a depth of 1000 meters, resulting in a sharp shift in gradient. Apart from this peak, there is a gradual decrease in thermal conductivity. Conversely, in the Kai Formation, thermal conductivity gradually increases up to 3.0 W/mK, continuing to increase into the Brygge Formation until it is above 3.0, and then a reversal occurs midway through the deposit. The values drop back to 3.0 W/mK. Both the Kai and Brygge Formations exhibit thermal conductivity values above the global average.

3.4.2 Southern Gimsan Basin

Most wells in this area are situated in the southern Gimsan Basin, contiguous to the Frøya High in the south and the Halten Terrace in the west. The two wells positioned in the more central-eastern part of the basin, proximal to the Froan Basin boundary, exhibit slight stratigraphic differences. However, the variations are not substantial, hence grouping them with the southern wells does not pose significant interpretational issues. Refer to Table 3.2 and figure 3.17 for more details.

In the Tertiary strata, all wells encounter the Nordland Group, reaching depths of approximately 1000 meters, with the Tertiary-Cretaceous boundary around 2000 meters. The thicknesses of the other Tertiary groups vary, but the Hordaland Group generally exhibits greater thickness than the Rogaland Group. Thermal conductivity data for the Nordland Group are only present in the Kai Formation. TC measurements for the Hordaland Group and Kai Formation are available only from wells 6407/7-3 and 6407/7-4 (figure 3.17). Besides these, only well 6407/8-1 has data for the Tang Formation.

Well Name	Linear Gradient (°C/km)	Location
6407/8-4A	41.8	Central East
6407/8-1	21.9	Central East
6407/7-5	40.1	Southeast
6407/7-9A	39.4	Southeast
6407/7-6	39.6	Southeast
6407/7-7S	41.0	Southeast
6407/7-3	40.1	Southeast
6407/7-2	40.6	Southeast
6407/7-4	41.0	Southeast
6407/10-1	38.6	Southeast
6407/10-2	33.2	Southeast

Table 3.2: Geothermal gradients in the central-eastern and southeastern parts of the Gimsan Basin. The central-eastern part abuts the Froan Basin within the Trøndelag Platform to the east, while the southeastern part borders the Frøya High to the south.

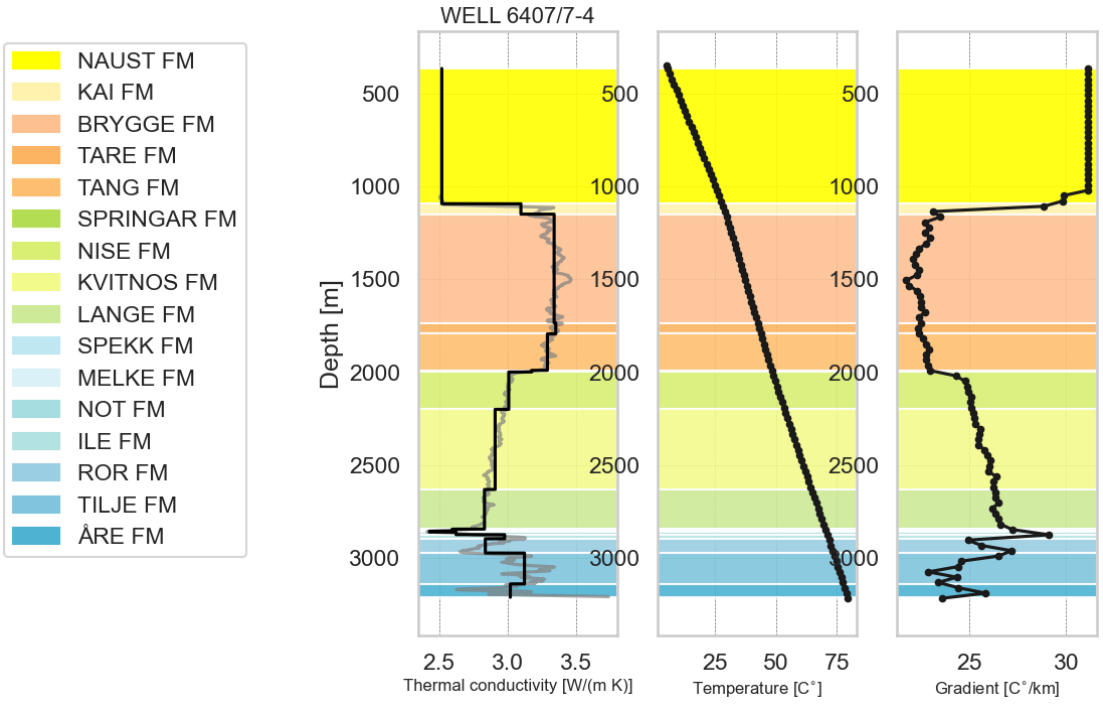

Figure 3.17: Thermal conductivity, temperature, and geothermal gradient versus depth for well 6407/7-4. The heat flow (q) ranges from 55 to 75 mW/m^2, and the estimated q value is 75 mW/m^2. The thermal conductivity above the data points (TC) ranges from 2.4 to 3.8 W/mK, and the estimated value is 2.4 W/mK. The measured Bottom Hole Temperature (BHT) is 122°C, whereas the estimated BHT is 79.8°C. The misfit in BHT values is -42.2°C, suggesting potential deviations from the assumed conditions or data inaccuracies. A total of 315 TC and q combinations were tested.

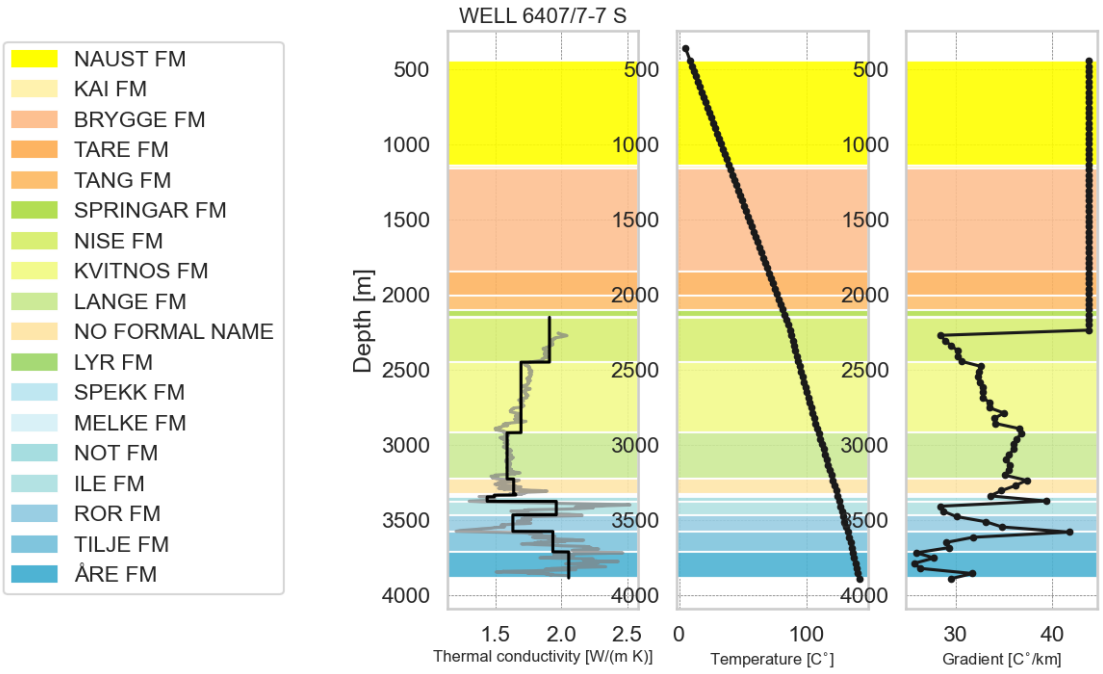

Figure 3.18: Thermal conductivity, temperature, and geothermal gradient versus depth for well 6407/7-7. The heat flow (q) ranges from 55 to 75 mW/m^2, and the estimated q value is 57 mW/m^2. The thermal conductivity above the data points (TC) ranges from 1.2 to 2.6 W/mK, and the estimated value is 1.3 W/mK. The measured Bottom Hole Temperature (BHT) is 141°C, whereas the estimated BHT is almost the same 141.2°C. The misfit in BHT values is -34.2°C, suggesting potential deviations from the assumed conditions or data inaccuracies. A total of 315 TC and q combinations were tested.

The Kai Formation exhibits high thermal conductivity values, leading to low geothermal gradients, around 3.00 W/mK and below 25°C/km, respectively. The formation's thickness varies between 0 to 200 meters across the wells. In the Hordaland Group, the Brygge Formation is the only unit present. Starting from the Kai Formation, thermal conductivity increases in the upper 500 meters, reaching almost 3.4 W/mK. The geothermal gradient decreases to near 20°C/km. For the lower part of the Brygge Formation and throughout the Rogaland Group, thermal conductivities and, therefore, the gradients generally remain constant at these levels, with the exception of a drop at the boundary between the Brygge and Tare Formations in well 6407/7-3. One well (6407/7-2) features a 600-meter-thick Kai Formation, where the Brygge Formation is absent. It appears that in locations where the Brygge Formation is thinner, the Kai Formation is correspondingly thicker, a relationship not correlated with geographical location. Despite these thickness variations, the thermal conductivities remain relatively consistent, aligning with the higher values observed in the global mean histograms for these formations.

Cretaceous

No well contains data from all Cretaceous formations. The Shetland Group and Lange Formation occur more frequently than the Lysing and Lyr formations. Data gaps are observed, primarily in the upper formations of the Cretaceous, especially in the Shetland Group. Among the 11 wells, nine have thermal conductivity data in Cretaceous formations, though not all groups are represented. Most wells lack data in the upper parts, while well 6407/8-1 lacks data in the lower part.

In the Shetland group, the Springar Formation is present in six wells, but only two have thermal conductivity data. The mean values are 2.97 and 3.18 W/mK , and while the layers are thin, a significant change in thermal conductivity is observed below and above the formation, with a gradient increase of 3-4 degrees per km. The Nise Formation is present in eight wells, with values around 3.0 W/mK. The thickness ranges from 100 to 200 m in most wells, significantly thicker than Springar Formation. There is a general pattern of reduction with depth, resulting in a gradual increase in the geothermal gradient. This trend continues in the Kvitnos Formation, with thermal conductivity values typically between 2.5-3.0 W/mK, without sudden drops or peaks.

In wells 6407/8-4S and 6407/7-7S (figure 3.18), the trend is similar, but values are significantly lower, with thermal conductivity values below 2.0 W/mK in the Nise Formation and approaching 1.5 in the Kvitnos formation. These wells exhibit overall lower thermal conductivities and higher gradients compared to other wells.

In the Cromer Knoll group, the Lysing Formation occurs infrequently, but in the two wells with data, thermal conductivities show a general decrease with depth, from around 2.8-2.5 W/mK, within the higher range of global distribution values. The trend is less

obvious in the Lange Formation, which displays more variation. The Lyr Formation has thin deposits where present, with values ranging from 1.6 - 3.0 W/mK. Lower values are observed in wells with low values in other Cretaceous formations.

Jurassic

In the Viking group, the Spekk Formation is most frequent, the Melke Formation is also quite common, while the Rogn Formation occurs less frequently. In the Fangst group, the Garn Formation is only present in well 6407/7-2, while the Not and Ile formations occur in most wells. The Båt group deviates from the stratigraphy, with formations occurring frequently, except the Tofte Formation, which is absent in this sub-area.

The Jurassic formations exhibit strong variation in thermal conductivity and gradient values, making the interpretation challenging. An interesting feature is that all Jurassic formations show values below 2.0 W/mK in wells 6407/8-1, -4, and 6407/7-7 S (figure 3.18), with some formations also in wells -9 and others in -5. These wells, being the northernmost within the sub-study area, suggest a pattern of lower conductivities.

The general pattern is a sharp increase in gradient at the base of the Cretaceous, where the Spekk Formation is encountered, typically followed by a sharp decrease when the Melke Formation is encountered. However, the Melke Formation sometimes contributes to a further decrease, indicating a strong heterolithic formation. The Båt group also shows strong variations. The overall Jurassic succession displays strong variation but a general reduction in gradient.

3.4.3 Trøndelag Platform – Froan Basin

The wells within the Froan Basin, which borders the southern Gimsan Basin to the west, are characterized by relatively shallow depths, with a maximum depth of approximately 2000 meters. Cretaceous sediments are nearly absent in many wells or, where present, the sedimentary succession is relatively thin. The thermal gradients exhibit stability within the Tertiary sediments, while the Jurassic strata show greater variability without a distinct pattern of gradient increase or decrease. Interestingly, the Molo Formation from the Nordland Group is observed in some wells, yet it does not demonstrate any specific patterns or noticeable changes within the formation.

Many wells in the Froan Basin exhibit lower TC than those in other sub-areas, particularly within the Jurassic formations. A consistent pattern observed throughout the entire study area is the reduction in TC in the Spekk Formation, which generally remains consistent with depth. Exceptions occur with peaks in the Rogn Formation, if encountered.
The wells in this area do not contain hydrocarbons and have a depth of around 4.0 - 4.5 km, drilled to Melke formation, except 6407/10-3 and 4, which are shallower, around 3 km, and drilled to the basement. There are fewer Jurassic formations here, as expected by the structural setting.

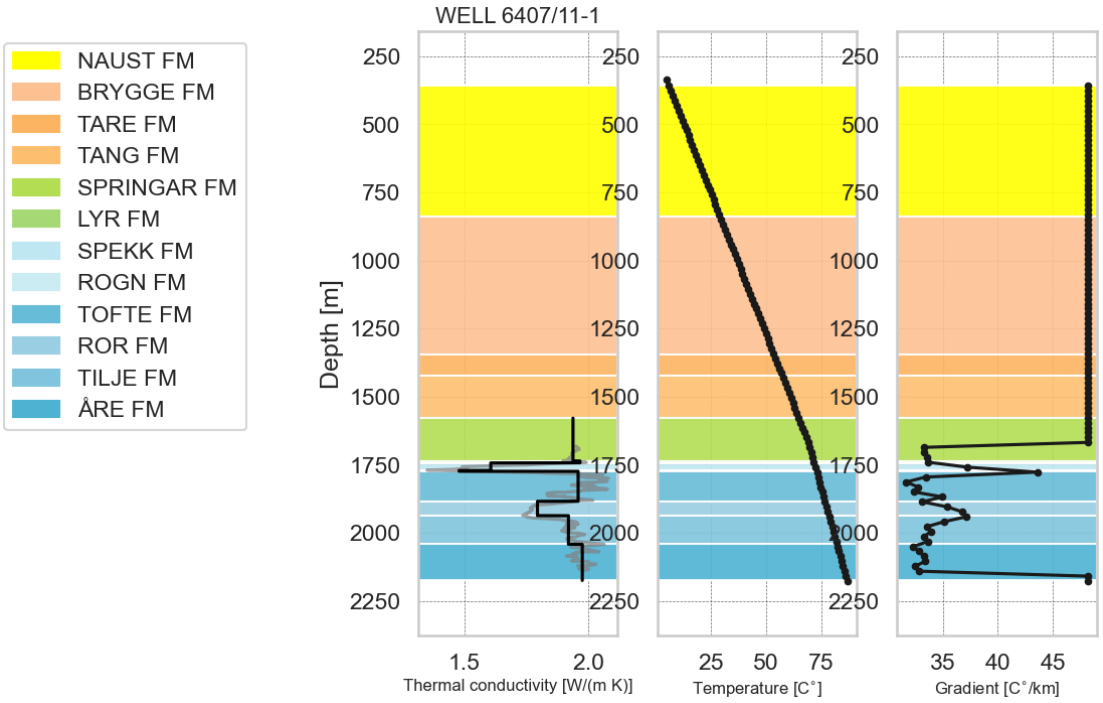

Figure 3.19: Thermal conductivity, temperature, and geothermal gradient versus depth for well 6407/11-1. The heat flow (q) ranges from 55 to 75 mW/m^2, and the estimated q value is 65 mW/m^2. The thermal conductivity above the data points (TC) ranges from 1.4 to 2.2 W/mK, and the estimated value is 1.4 W/mK. The measured Bottom Hole Temperature (BHT) is 87°C, and the estimated BHT is the same. A total of 189 TC and q combinations were tested.

Well	Linear Gradient (°C/km)	Province
6407/9-7	30.0	Froan Basin
6407/9-2	28.2	Froan Basin
6407/9-1	42.2	Froan Basin
6407/9-5	28.7	Froan Basin
6407/12-3	39.1	Froan Basin
6407/12-1	42.9	Froan Basin
6407/12-2	37.9	Froan Basin
6407/11-1	44.6	Froan Basin
6407/8-2	44.2	Froan Basin

Table 3.3: The Froan Basin borders the southern Gimsan Basin towards the west. The table summarizes the geothermal gradients of wells within this sub-area.

Well Name	Linear Gradient (°C/km)	Location
6407/10-3	33,9	Frøya High/Froan Basin
6407/10-4	38,5	Frøya High/Gimsan Basin
6406/12-2	35,2	Gimsan Basin
6406/12-5S	37,0	Gimsan Basin
6406/12-1S	40,1	Gimsan Basin
6406/12-4A	37,1	Frøya High South

Table 3.4: Central east part of Gimsan basin borders Froan basin in Trøndelag platform to the east, and the southeast part of Gimsan basin borders Frøya High in the south.

Tertiary

The Naust, Brygge, and Kai formations are similar to wells in the southern Gimsan basin in terms of thickness and depth. None of the wells have TC data, so the interpretation is limited. Limited data from the Rogaland group show mean TC values around 2.3 W/mK in well 6407/10-4, slightly below the mean value for both formations. The Tare Formation also shows slightly higher values than the Tang Formation, opposite to the global trend. Well 6407/10-3 exhibits no clear trend in the gradient, with variations of around 25 °C/km.

Cretaceous

The thicknesses of the Cretaceous formations vary, with the full Cretaceous succession showing thicknesses over 1000m, except for wells 10-3 and 10-4. As discussed in the lithology section, these wells are drilled to the basement and have relatively thin Cretaceous sediment. Only a very thin layer of the Cromer Knoll (Lange and Lyr formations) group is present. These two wells show an increasing gradient with depth and decreasing TC values within the Cretaceous succession. This is distinct for these two wells in this

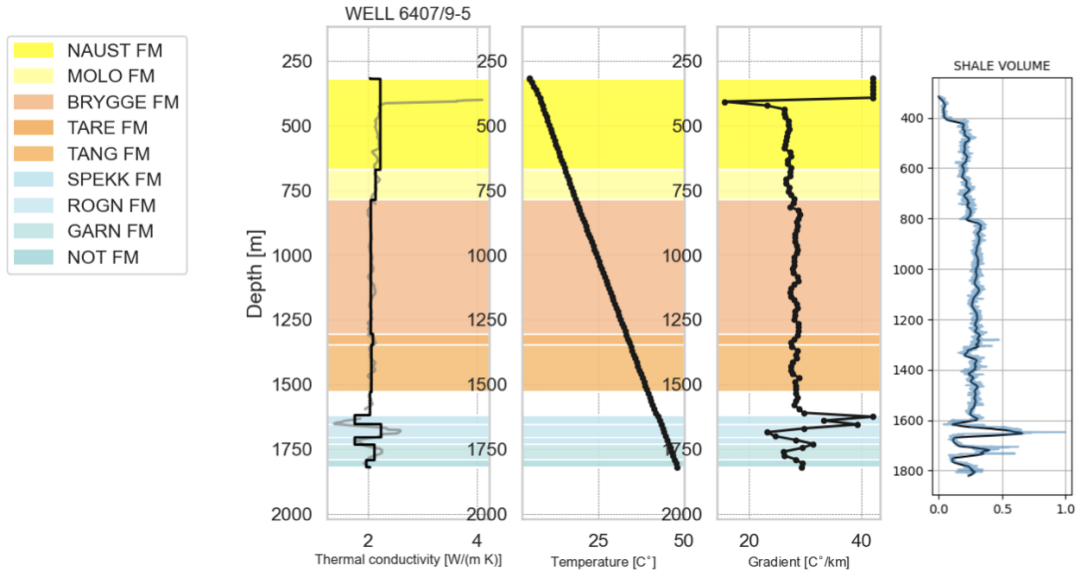

Figure 3.20: Thermal conductivity, temperature, and geothermal gradient versus depth for well 6407/9-5. The heat flow (q) ranges from 55 to 75 mW/m^2, and the estimated q value is 58 mW/m^2. The thermal conductivity above the data points (TC) ranges from 1.4 to 2.1 W/mK, and the estimated value is 1.4 W/mK. The measured Bottom Hole Temperature (BHT) is 47°C, and the estimated BHT is the same. A total of 609 TC and q combinations were tested.

group. The mean TC values for the Cretaceous sediments in well 6407/10-3 are higher than the global mean, around 2.8-3.0 W/mK, while the values are below the global mean in well 6407/10-4, ranging between 1.9 - 2.5. The gradient in 10-4 is towards 40 °C/km at the base Cretaceous, significantly higher than 10-3. Many wells show a sharp decrease in TC values at the base Cretaceous layer, often in the Lyr Formation.

Jurassic

The only Jurassic deposits in well 6407/10-3 and 4 are very thin layers of the Spekk Formation, with TC values of 2.57 and 1.83 W/mK, respectively. However, this thin layer results in a significant jump in the gradient. No wells have Båt or Fangst group deposits, and the Spekk Formation is everywhere thin. Some wells show gradients and TC values that vary a lot with depth, others show a strong increase in gradient, and others show a strong decrease in gradient.

Triassic

There are thick Triassic deposits in wells 10-4 and 10-3. Thermal conductivities increase from around 2.0 to 2.5 W/mK in 10-4, but this still results in a decrease in gradient to around 25°C/km. In 10-3, there is variation and no clear decrease or increase of thermal gradient, resulting in a gradient ranging between 25-30 °C/km.

3.4.4 Northeast Gimsan Basin, Including Ellingråsa Graben and North Trøndelag Platform

Identifying a representative well in this area was challenging due to the scarcity of data. Despite this, figures 3.21 and 3.22 were selected based on the consistency of the available data. They also represent the most western and most eastern wells in the subarea, respectively.

The lithostratigraphy and thicknesses of the wells in this area are generally consistent, especially in the upper Tertiary layers. Due to limited data, these formations will not be discussed in detail. The Brygge, Tare, and Tang formations exhibit high thermal conductivities in the wells where they occur, leading to a general decrease in the geothermal gradient until the Cretaceous boundary. Most wells demonstrate a gradual increase in gradients with depth in the Cretaceous layers, followed by a sudden jump at the onset of the Jurassic, before exhibiting variability.

Well 6407/6-1, situated on the Trøndelag Platform, reveals a very thin Cretaceous deposit, which is also the case in many wells in the Froan Basin. Similarly, the Cretaceous is relatively thin in well 6407/6-6, which lies on the boundary of the Trøndelag Platform and is relatively close to well 6407/6-1. However, the latter well presents a less substantial Jurassic deposit. The thermal conductivity values of these two wells are quite similar in the Jurassic, varying between 2.0 and 2.5 W/mK, which is consistent with most wells in this subarea.

Well Name	Linear Gradient (°C/km)	Location
6407/2-5S	36.5	Ellingråsa Graben
6407/2-6S	38.8	Ellingråsa Graben
6407/3-1S	39.8	Ellingråsa Graben
6407/6-1	37.9	Trøndelag Platform
6407/6-6	38.5	Trøndelag Platform
6407/6-7S	41.9	Trøndelag Platform
6407/5-2S	40.9	Trøndelag Platform
6407/5-1	37.0	Trøndelag Platform

Table 3.5: The northeast part of Gimsan Basin is adjacent to the Trøndelag Platform to the east and bounded by the Ellingråsa Graben to the north.

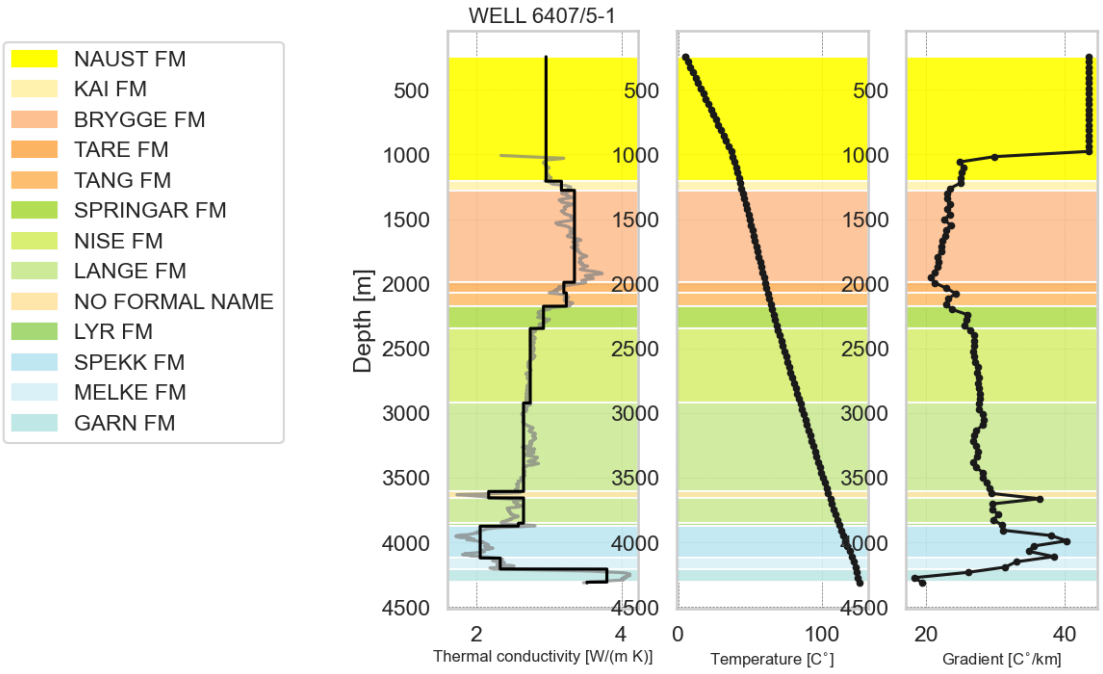

Figure 3.21: Thermal conductivity, temperature, and geothermal gradient versus depth for well 6407/5-1. The heat flow (q) ranges from 55 to 75 mW/m^2, and the estimated q value is 75 mW/m^2. The thermal conductivity above the data points (TC) ranges from 1.7 to 4.1 W/mK, and the estimated value is 1.7 W/mK. The measured Bottom Hole Temperature (BHT) is 155°C, whereas the estimated BHT is 125.1°C. The BHT misfit of -29.9°C suggests potential deviations from the assumed conditions or data inaccuracies. A total of 525 TC and q combinations were tested. 125.1°C.

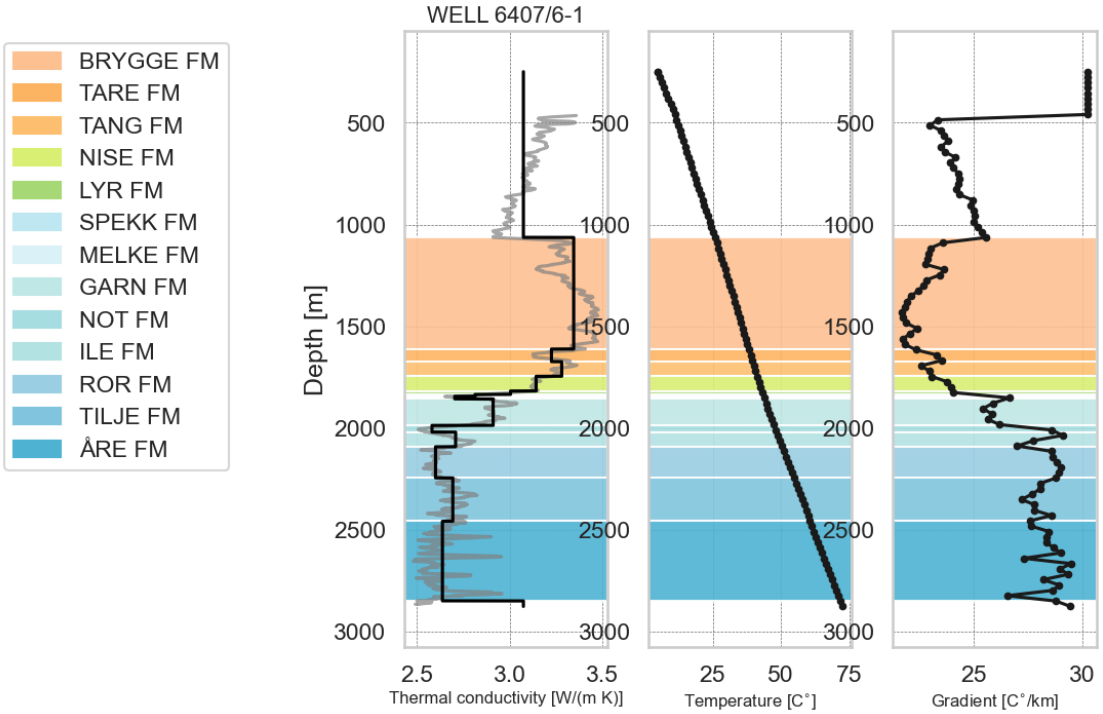

Figure 3.22: Thermal conductivity, temperature, and geothermal gradient versus depth for well 6407/6-1. The heat flow (q) ranges from 55 to 75 mW/m^2, and the estimated q value is 75 mW/m^2. The thermal conductivity above the data points (TC) ranges from 2.5 to 3.5 W/mK, and the estimated value is 2.5 W/mK. The measured Bottom Hole Temperature (BHT) is 105°C, whereas the estimated BHT is 72.6°C. The BHT misfit of -32.4°C suggests potential deviations from the assumed conditions or data inaccuracies. A total of 231 TC and q combinations were tested. 125.1°C.

Discussion

4.1 Temperature data

The assumption that BHT data from NPD represents the equilibrium formation temperature, introduces some uncertainties in our analysis. Pascal (2015) avoided BHT temperatures and only utilized wells with available DST temperatures. For well 6406/3-1, completion reports state a DST temperature of 140 °C, and a BHT of 169 °C. However, a comparison of our results with Pascal (2015) reveals a significantly higher heat flow value in this study, attributed to the difference in BHT temperatures (169 vs. 140 °C). Aligning with Goutorbe et al. (2007), Pascal (2015) argues that the lack of information in BHT corrections renders these data unreliable, favoring DST temperatures. The completion report for this specific well indicates a DST temperature of 140 °C, though not at the bottom hole. While this may suggest the appropriateness of the BHT temperature of 169 °C, the substantial discrepancy of our heat flow values compared to (Pascal, 2015) and other estimates raises doubts about BHT. In cases where DST temperatures are available, it can be better to use these.

Brigaud et al. (1992) reconstructed thermal gradients using corrected BHT measurements and DST temperatures. They found a relatively higher gradient for subsets using DST, raising doubts about the reliability of DST temperatures, particularly in gas reservoirs.

For the purpose of this study, the absence of data on time since circulation for wireline BHT measurements and uncertainty about the applicable wells, make corrections for BHT impractical. In essence, the unreliability of the BHT data could potentially introduce a critical source of error.

4.2 Thermal conductivity analysis

4.2.1 Rock Type Classification

The classification of rock types in this study employed an algorithmic approach. While this method is generally effective, it introduced certain uncertainties due to the inherent

diversity in rock compositions. An unexpectedly high proportion of carbonates relative to clastics was observed. This outcome, potentially influenced by a considerable number of NaN values, raises questions about the algorithm's precision in specific contexts. Nonetheless, the employed equations account for a degree of compositional variability, offering a realistic estimate in many cases.

However, a notable exception arises in the presence of evaporites, which are not considered in the model. The synthetic rock composition of evaporites(Table 1.2) exhibit less compositional variation. If evaporite deposits, such as salt, are present but unaccounted for, the resulting thermal conductivity (TC) values could be underestimated. This issue is particularly relevant for Triassic deposits. However, there is no direct evidence of such underestimation in the data, suggesting the absence of significant evaporite deposits.

4.2.2 Uncertainties and validation of equations

Applying the most accurate equations based on the data availability resulted in negative TC values. The cause of these negative values is not entirely clear, but an examination of the equations suggests that they may not adequately account for high porosities. While designed to handle porosities up to 30 percent, these equations are also known to be sensitive to porosity measurements (Fuchs et al., 2015). This could indicate either an overestimation of porosity in the well logs or porosities that exceed the equations' operational range.

The issue was addressed by testing alternative equations, ultimately selecting one with lower R-squared values for the clastic intervals. This choice implies potential errors. Moreover, variables such as organic content, degree of sorting, and non-sedimentary sequences (e.g., basement rocks, volcanic tuffs) are not directly incorporated in these equations, potentially leading to errors in specific scenarios. Despite these uncertainties, the observed variations in thermal conductivity align well with anticipated values for different rock types Table 1.1, suggesting that these uncertainties did not significantly impact the overall findings.

4.3 Heat flow considerations

Our assumption of a constant heat flow may not fully capture the dynamic nature of geological processes, including paleoclimatic effects, erosion, and compaction. Additionally, factors such as radiogenic heat production and convection, particularly relevant in hydrocarbon-rich areas with organic content and shale presence, are not considered. The simplification of heat flux as solely conductive might contribute to an overestimation of heat flow values, influencing the interpretation of thermal conductivity and geothermal gradient correlations. Therefore, our findings do not necessarily reflect accurate scenarios.

4.4 Geothermal gradient implications

The inverse relationship between geothermal gradients and thermal conductivity values gives higher temperatures in formations with lower thermal conductivities, depending on the underlying heat flow conditions. Notably, thermal conductivities demonstrated correlation within individual wells and not only across different formations, indicating both vertical and lateral heterogeneities in the subsurface. There are substantial differences between and within the formations, as well as between and within wells. However, there are some patterns, such as the significant variation of thermal gradient / conductivity in the Jurassic formations, compared to a more constant pattern in Cretaceous deposits. Despite variations in thermal conductivities between wells, there is a general pattern of relative changes of thermal conductivity between formations. This is confirmed in figures 3.5 and 3.9, which shows the complexity of the thermal regime within the study area. The generally higher TC values in the Cromer Knoll Group compared to the Shetland Group figure 3.9 suggest that the former may consist of rocks with a higher thermal conductivity, resulting in less geothermal gradients and geothermal potential. Conversely, the varying TC values in the Spekk Formation figure 3.5 highlight the need for a more flexible approach when interpreting thermal data, as localized geological processes could significantly affect the area's thermal properties.

4.4.1 Comparison to linear gradient

Due to assumptions made in this study, comparing the estimated gradients directly to the linear gradient in terms of temperature regime is not accurate. However, the results of the study clearly demonstrate a more realistic situation. In fact, the variation in thermal gradient depends on lithology, structural setting, as well as other factors.

4.4.2 Implications for geothermal potential

The overall results shows several areas with potential for geothermal exploitation in terms of the computed thermal conductivity values and the estimated heat flow values. The boundary limits for heat flow values should be within an acceptable range, which is further supported by comparing them to previous heat flow studies conducted in the same region (Pascal, 2015). However, there are also areas where the thermal conductivity values are higher than expected within the given heat flow range. This may result in geothermal gradients that do not reach the required temperatures for geothermal utilization. This knowledge is valuable for determining the areas with most geothermal potential.

The observed non-linear nature of geothermal gradients, particularly in deeper wells, suggests a complex interplay of factors influencing geothermal potential. The Cretaceous successions emerged as the most promising for geothermal exploration. However, high gradients in thinner Jurassic deposits underscore the significance of local geological conditions.

When considering geothermal exploration and the potential for energy extraction, these findings emphasize the importance of accounting for the spatial variability of thermal properties. Regions with uniform and higher TC values, may be more predictable and thus more favorable for geothermal projects. However, the complexities observed in certain formations require careful analysis to understand the impact of heterogenous lithologies and thermal conductivities on the geothermal gradient and overall energy potential.

4.5 Improvements

4.5.1 Improving thermal conductivity estimates for intervals with missing data

Utilizing global mean values for formations with missing data, rather than relying on constant values estimated from boundary values within specific wells, initially appeared as a superior approach. However, due to significant inter-well variations in thermal conductivities, this method may require further refinement. A promising approach could involve combining global formation-specific conductivity distributions with the methodology used in this study to estimate TC values within formations, rather than across entire intervals with missing data. This would not only consider the well-specific value range but also the unique characteristics of each formation. Ideally, avoiding constant values altogether would best reflect the complex reality.

4.5.2 Enhancing accuracy of thermal conductivity estimates

Integrating additional methods for rock classification could reduce uncertainties and yield more realistic thermal conductivity values. A more detailed interpretation of well logs, compared to the synthetic rocks used in the equations, would be beneficial. Additionally, a thorough analysis of the differences within thermal conductivity equations could better accommodate high porosity values and other specific geological conditions. Access to more comprehensive data would allow for the use of more accurate equations, potentially improving their validation.

4.5.3 Correlation and interpretation of temperature differences and factors affecting the thermal regime

Developing temperature maps based on the geothermal gradient at various depths could enhance understanding of the factors predominantly affecting thermal regime variations. To create accurate maps, it is essential to first ensure more reliable thermal conductivity estimates, especially if data gaps persist.

4.5.4 Reconstructing geothermal gradients with enhanced accuracy

Considering non-constant heat flow values could improve accuracy. This might involve (a) assuming an increase in heat flow with depth, (b) using a lower heat flow value at shallow depths to account for paleoclimatic effects, or (c) estimating heat flow based on boundary conditions, such as basement and sea floor heat flow values.

Conclusion

The primary objective of this study was to explore and analyze the geothermal gradients in the Froan and Gimsan basins, with a focus on using well log data for a better understanding of the geothermal properties in these areas. This exploration is key for evaluating the geothermal potential and contributes to a broader understanding of the geological and geophysical characteristics of the Norwegian Sea.

The findings of this thesis demonstrate that the geothermal gradient in these basins is non-linear and is significantly influenced by subsurface heterogeneities. Thermal conductivity is emphasized, as a critical parameter in heat conduction. This study reveals that lithological heterogeneities in sedimentary basins strongly affect the thermal distribution, making necessary localized approaches in geothermal exploration. Factors such as structural setting, basement composition, and variations in heat flow emerged as crucial in shaping the thermal characteristics of the studied region.

The use of the approach suggested by Fuchs et al. (2015) for evaluating thermal conductivity using well log responses allows for detailed insights into a property that is continuous and critical for a better determination of the thermal regime. This method provides direct estimation without the need for laboratory tests, enhancing the efficiency and accuracy of geothermal assessments.

While the findings confirm the potential for geothermal energy in the area, they also caution against generalized assumptions due to the observed heterogeneities. Selecting the appropriate formation or well for exploration requires careful consideration. The lack of comprehensive data and the necessary simplifications in the model mean that no specific area can be definitively recommended. However, the study does provide valuable estimates of thermal conductivity, an important parameter in understanding the geothermal potential.

In conclusion, this thesis contributes to the field of geothermal energy by highlighting the complex nature of subsurface thermal regimes and the critical role of thermal conductivity. The findings underscore the need for more detailed and localized studies in future geothermal exploration efforts.

Bibliography

Bagdassarov, N. (2021). *Fundamentals of Rock Physics* (1st ed.). Cambridge University Press. https://doi.org/10.1017/9781108380713

Blystad, P., Brekke, H., Larsen, T. B., Skogseid, J., Tørudbakken, B., & Færseth, R. B. (1995). Structural Elements of the Norwegian Continental Shelf. *8*, 45.

Boden, D. R. (2017). *Geologic Fundamentals of Geothermal Energy*. CRC Press.

Brekke, H., & Riis, F. (1987). Tectonics and basin evolution of the Norwegian shelf between 62°N and 72°N. *Norsk Geologisk Tidsskrift*, *67*, 295–322.

Brigaud, F., Vasseur, G., & Caillet, G. (1992). Thermal state in the north Viking Graben (North Sea) determined from oil exploration well data. *GEOPHYSICS*, *57*(1), 69–88. https://doi.org/10.1190/1.1443190

Dalland, A., Worsley, D., & Ofstad, K. (1998). A lithostratigraphic scheme for the Mesozoic and Cenozoic succession offshore mid- and northern Norway.

Elders, W., & Moore, J. (2016). Geology of geothermal resources. *Geothermal Power Generation* (pp. 7–32). Elsevier. https://doi.org/10.1016/B978-0-08-100337-4.00002-4

English, J. M., English, K. L., Dunphy, R. B., Blake, S., Walsh, J., Raine, R., Vafeas, N. A., & Salgado, P. R. (2023). An Overview of Deep Geothermal Energy and Its Potential on the Island of Ireland. *41*(2), 33–43. https://doi.org/10.3997/1365-2397.fb2023009

Evans, T. R., & Coleman, N. C. (1974). North Sea Geothermal Gradients. *Nature*, *247*(5435), 28–30. https://doi.org/10.1038/247028a0

Færseth, R. (2021). Structural geology and basin development of the Norwegian Sea. https://doi.org/10.17850/njg100-4-1

Fuchs, S., Balling, N., & Förster, A. (2015). Calculation of thermal conductivity, thermal diffusivity and specific heat capacity of sedimentary rocks using petrophysical well logs. *Geophysical Journal International*, *203*(3), 1977–2000. https://doi.org/10.1093/gji/ggv403

Goutorbe, B., Lucazeau, F., & Bonneville, A. (2007). Comparison of several BHT correction methods: A case study on an Australian data set. *Geophysical Journal International*, *170*(2), 913–922. https://doi.org/10.1111/j.1365-246X.2007.03403.x

Grotzinger, J. P., & Jordan, T. H. (2014). *Understanding Earth* (7th ed.). W.H. Freeman; Company.

Hearst, J. R., Nelson, P. H., & Pailett, F. L. (1988). *Well Logging for Physical Properties* (2nd ed.). John Wiley & Sons, Ltd.

Kauerauf, A. I., & Hantschel, T. (2009). *Fundamentals of Basin and Petroleum Systems Modeling*. Springer Berlin Heidelberg.

Labus, M., & Labus, K. (2018). Thermal conductivity and diffusivity of fine-grained sedimentary rocks. *Journal of Thermal Analysis and Calorimetry*, *132*(3), 1669–1676. https://doi.org/10.1007/s10973-018-7090-5

Lien, T. (2005). From rifting to drifting: Effects on the development of deep-water hydrocarbon reservoirs in a passive margin setting, Norwegian Sea. *Norwegian Journal of Geology*, *85*, 319–332.

Lundin, E. R., Polak, Bøe, R., Zweigel, & Lindeberg, E. (2005). Storage potential for CO2 in the Froan Basin area of the Trøndelag Platform, Mid-Norway [Publisher: Unpublished]. https://doi.org/10.13140/RG.2.2.36601.26723

Mello, V. L. D., & Lupinacci, W. M. (2022). Mineralogy based classification of carbonate rocks using elastic parameters: A case study from Buzios Field. *Journal of Petroleum Science and Engineering*, *209*. https://doi.org/10.1016/j.petrol.2021.109962

Nolan, C. (2021). Geothermal Energy and Ice an unlikely alliance? Insights from temperature data on the Norwegian Continental Shelf [Publisher: Unpublished]. https://doi.org/10.13140/RG.2.2.24613.22240

NPD. (2023). *Factpages - Wellbore Information* (Webpage). Retrieved November 16, 2023, from https://factpages.npd.no/nb-no/wellbore/PageView/Exploration/All

Pascal, C. (2015). Heat flow of Norway and its continental shelf. *Marine and Petroleum Geology*, *66*, 956–969. https://doi.org/10.1016/j.marpetgeo.2015.08.006

Rider, M., & Kennedy, M. (2014). *The Geological Interpretation of Well Logs* (3rd ed.). Rider-French Consulting Ltd.

Riis, F., Mujezinović, J., Halland, E. K., Bjørøen, A., & Goa, R. (2014). *CO Storage Atlas: Norwegian Continental Shelf* [OCLC: 1025329042]. Norwegian Petroleum Directorate (NPD).

Wang, Y., Wang, Z., Shi, L., Rong, Y., Hu, J., Jiang, G., Wang, Y., & Hu, S. (2021). Anisotropic Differences in the Thermal Conductivity of Rocks: A Summary from Core Measurement Data in East China. *Minerals*, *11*(10), 1135. https://doi.org/10.3390/min11101135